From Stream Flows to Cash Flows: Leveraging Evolutionary Multi-Objective Direct Policy Search to Manage Hydrologic Financial Risks

Andrew L. Hamilton[1,1], Gregory W. Characklis[2,2], and Patrick M. Reed[3,3]

[1]University of North Carolina at Chapel Hill
[2]University of North Carolina - Chapel Hill
[3]Cornell University

November 30, 2022

Abstract

Hydrologic variability can present severe financial challenges for organizations that rely on water for the provision of services, such as water utilities and hydropower producers. While recent decades have seen rapid growth in decision-support innovations aimed at helping utilities manage hydrologic uncertainty for multiple objectives, support for managing the related financial risks remains limited. However, the mathematical similarities between multi-objective reservoir control and financial risk management suggest that the two problems can be approached in a similar manner. This paper demonstrates the utility of Evolutionary Multi-Objective Direct Policy Search (EMODPS) for developing adaptive financial risk management policies in the context of hydropower production in a snow-dominated region. These policies dynamically balance a portfolio, consisting of snowpack-based financial hedging contracts, cash reserves, and debt, based on evolving system conditions. Performance is quantified based on four conflicting objectives, representing the classic tradeoff between "risk" and "return" in addition to decision-makers' unique preferences towards different risk management instruments. The dynamic policies identified here significantly outperform static management formulations that are more typically employed for financial risk applications in the water resources literature. Additionally, this paper combines visual analytics and information theoretic sensitivity analysis to help decision-makers better understand how different candidate policies achieve their comparative advantages through differences in how they adapt to real-time information. The methodology developed in this paper should be applicable to any organization subject to financial risk stemming from hydrology or other environmental variables (e.g., wind speed, insolation), including electric utilities, water utilities, agricultural producers, and renewable energy developers.

From Stream Flows to Cash Flows: Leveraging Evolutionary Multi-Objective Direct Policy Search to Manage Hydrologic Financial Risks

Andrew L. Hamilton[1,2], Gregory W. Characklis[1,2], and Patrick M. Reed[3]

[1]Department of Environmental Sciences and Engineering, Gillings School of Global Public Health, University of North Carolina at Chapel Hill, Chapel Hill, NC, USA
[2]Center on Financial Risk in Environmental Systems, Gillings School of Global Public Health, UNC Institute for the Environment, University of North Carolina at Chapel Hill, Chapel Hill, NC, USA
[3]Department of Civil and Environmental Engineering, Cornell University, Ithaca, NY, USA

Key Points:

- Reservoir control and financial risk management share a common multi-objective decision structure and can be optimized using similar methods
- Evolutionary Multi-Objective Direct Policy Search (EMODPS) is used to develop financial risk management policies for a hydropower producer
- Information theoretic sensitivity analysis and visual analytics are used to build intuition about how policies adapt to changing conditions

Corresponding author: Andrew L. Hamilton, andrew.hamilton@unc.edu

Abstract

Hydrologic variability can present severe financial challenges for organizations that rely on water for the provision of services, such as water utilities and hydropower producers. While recent decades have seen rapid growth in decision-support innovations aimed at helping utilities manage hydrologic uncertainty for multiple objectives, support for managing the related financial risks remains limited. However, the mathematical similarities between multi-objective reservoir control and financial risk management suggest that the two problems can be approached in a similar manner. This paper demonstrates the utility of Evolutionary Multi-Objective Direct Policy Search (EMODPS) for developing adaptive policies for managing the drought-related financial risk faced by a hydropower producer. These policies dynamically balance a portfolio, consisting of snowpack-based financial hedging contracts, cash reserves, and debt, based on evolving system conditions. Performance is quantified based on four conflicting objectives, representing the classic tradeoff between "risk" and "return" in addition to decision-makers' unique preferences towards different risk management instruments. The dynamic policies identified here significantly outperform static management formulations that are more typically employed for financial risk applications in the water resources literature. Additionally, this paper combines visual analytics and information theoretic sensitivity analysis to help decision-makers better understand how different candidate policies achieve their comparative advantages through differences in how they adapt to real-time information. The methodology developed in this paper should be applicable to any organization subject to financial risk stemming from hydrology or other environmental variables (e.g., wind speed, insolation), including electric utilities, water utilities, agricultural producers, and renewable energy developers.

Keywords

hydropower, water resources, financial risk, direct policy search, reservoir control, global sensitivity analysis

1 Introduction

Reservoir control and financial risk management share strong similarities. The principal task in each is to reduce the risk of negative impacts from variable inflows (either hydrologic flows or cash flows), through the use of a buffer stock (either a reservoir or a reserve fund) that is filled in times of abundance and drawn down in times of scarcity (Figure 1). Other risk management tools may also be used to limit the impact of low-flow periods, but at a cost (e.g., water desalination or demand management for streamflow deficits, and borrowing or financial hedging for cash flow deficits). In both cases, the manager must make decisions under an array of uncertainties, and may need to navigate tradeoffs between conflicting objectives (e.g., flood control vs. water supply for reservoir control, risk vs. cost for financial risk management). And in both cases, as systems dynamically evolve, managers will have to adapt to new information as it becomes available. In other words, reservoir control and financial risk management can be formulated as very similar Markov Decision Processes (MDPs) (Bertsekas, 2019; Powell, 2019), whether managers attempt to solve this problem explicitly, using programmatic approaches such as stochastic dynamic programming, or implicitly, relying on expert specified rules. Additionally, reservoir control and financial risk management are strongly interdependent activities for water-reliant organizations in the Food-Energy-Water Nexus, such as hydropower producers, municipal water utilities, and irrigation districts (Cai, Wallington, Shafiee-Jood, & Marston, 2018; D'Odorico et al., 2018; Scanlon et al., 2017). Such organizations rely on water for the provision of services, and as a result, their revenues and/or costs can be highly dependent on hydrologic inflows (Blomfield & Plummer, 2014; Larson, Freedman, Passinsky, Grubb, & Adriaens, 2012). This suggests that an understanding of complex water resource system dynamics can be used to better characterize and adaptively manage financial risks borne by water-reliant organizations.

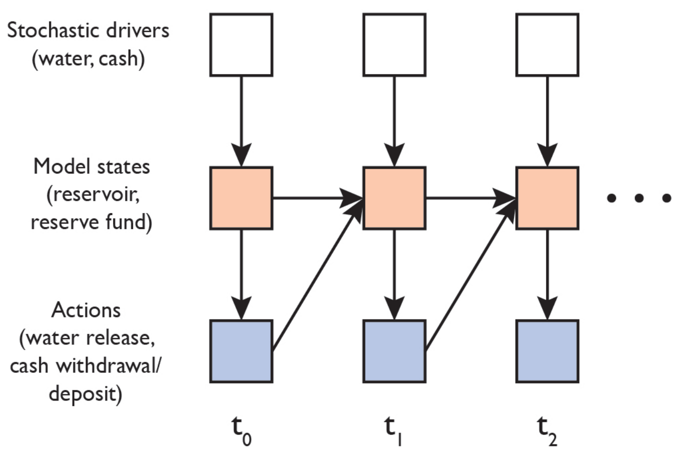

Figure 1. A simple reservoir model and a simple cash flow model share the same underlying decision structure.

Water resource systems researchers have developed a broad range of strategies for dynamically managing reservoir operations in the face of uncertain hydrometeorology and demands (see reviews by Castelletti, Pianosi, and Soncini-Sessa (2008); Labadie (2004); Macian-Sorribes and Pulido-Velazquez (2019); Yeh (1985)), but Stochastic Dynamic Programming (SDP) and its many derivatives have been the most popular. The problem is formulated as an MDP in which a decision-maker must make sequential decisions based on the stochastically evolving state of the system. Each action affects the immediate cost/reward as well as the future state of the system. In SDP, this recursion is used to find optimal operating rules, in the form of a discrete policy table, using the Bellman Equation (Bellman, 1957). However, despite its widespread use, SDP suffers from a number of limitations that reduce its applicability to large, complex, multi-objective problems where operations are evaluated using stochastic simulations (see discussion in Giuliani, Castelletti, Pianosi, Mason, and Reed (2016)).

A variety of approximation methods have been developed to overcome these challenges, such as approximate dynamic programming, reinforcement learning, and model predictive control (Bertsekas, 2019). Direct Policy Search (DPS) (Rosenstein & Barto, 2001), or parameterization-simulation-optimization (Koutsoyiannis & Economou, 2003), has become increasingly popular in the field of water resources systems analysis (Macian-Sorribes & Pulido-Velazquez, 2019). DPS is an approximation in policy space (Powell, 2019), wherein the optimal operating policy is assumed to lie in the space of a certain parametric family of functions, and the policy parameters are optimized rather than the decisions themselves (i.e., optimizing state-aware adaptive rule systems instead of specific actions). This drastically reduces the "curse of dimensionality" that limits the tractability of large SDP problems. Additionally, DPS allows for "model-free" representation of stochastic inputs, meaning that observational data, synthetically generated data, and process-based simulation model output can all be used in lieu of explicit probability distributions (Desreumaux, Côté, & Leconte, 2018; Giuliani, Quinn, Herman, Castelletti, & Reed, 2018). A simulation-based approach to optimization also allows for flexible construction of mixed multi-objective formulations (Giuliani et al., 2016; Kasprzyk, Reed, & Hadka, 2016; Quinn, Reed, & Keller, 2017). In Evolutionary Multi-Objective Direct Policy Search (EMODPS) (Giuliani, Herman, Castelletti, & Reed, 2014), the policies are parameterized with a non-linear approximating network and optimized using a multi-objective evolutionary algorithm (MOEA). EMODPS has been deployed to solve complex reservoir operations problems (multiple reservoirs; multiple, mixed objectives; and model-free information) that would be untenable using a traditional SDP approach (Denaro, Anghileri, Giuliani, & Castelletti, 2017; Giuliani, Pianosi, & Castelletti, 2015; Quinn et al., 2018; Zatarain Salazar, Reed, Quinn, Giuliani, & Castelletti, 2017).

To complement algorithmic search strategies, water resources researchers have developed an assortment of computational tools to help decision-makers better understand their options. This is especially important in multi-objective contexts, where optimization results in a multitude of solutions representing the optimal tradeoffs between conflicting objectives (the Pareto set), rather than a single "best" policy. As the dimensionality of the Pareto set grows, it becomes increasingly difficult to conceptualize. High-dimensional visualization, solution brushing, and other visual analytic techniques can help decision-makers to better understand the complex tradeoffs in their system and choose the solution that best suits their needs (Herman, Zeff, Reed, & Characklis, 2014; Huskova, Matrosov, Harou, Kasprzyk, & Lambert, 2016; Kollat & Reed, 2007). These tools can also help decision-makers to refine their conceptualization of the problem through iterative reformulation (Castelletti & Soncini-Sessa, 2006; Giuliani, Herman, et al., 2014; Kasprzyk, Reed, Characklis, & Kirsch, 2012). Visual analytics are especially powerful when combined with global sensitivity analyses that probe the impacts of key uncertainties on system performance (Iooss & Lemaître, 2015; Pianosi et al., 2016; Saltelli, Tarantola, & Campolongo, 2000). These tools can be used to "open the black box" of non-linear approximating networks and help decision-makers to better understand how the optimal operating policies adapt to changing conditions (Quinn, Reed, Giuliani, & Castelletti, 2019). In this way, visual analytics and sensitivity analysis can help to build trust between water resources modelers and real-world stakeholders. Although water resources practitioners in general have been slow to adopt computational decision support tools such as MOEAs, visual analytics, and global sensitivity analysis (Basdekas, 2014; Brown et al., 2015), a growing number of real-world use cases suggests that this may be changing (Basdekas & Hayslett, 2021; Moallemi, Kwakkel, de Haan, & Bryan, 2020; Smith, Kasprzyk, & Dilling, 2019; Wild, Reed, Loucks, Mallen-Cooper, & Jensen, 2019; Wu et al., 2016).

Many organizations such as water utilities and hydropower producers rely on water for the provision of services. During drought, these organizations can experience reduced revenues and/or increased costs (Hughes et al., 2014; Larson et al., 2012). For example, an electric utility with reduced hydropower capacity during drought will have less electricity to sell (reduced revenues) and/or be forced to purchase more expensive replacement power from other generators (increased costs). Similarly, a water utility experiencing supply shortfalls will typically implement demand management measures (reduced revenues) and/or water purchases from other utilities or irrigators (increased costs). These measures can result in severe cash flow deficits that leave an organization at risk of defaulting on its obligations (e.g., debt service, operations and maintenance) (Ceres, 2017; Leurig, 2010). Water utilities and hydropower-reliant electric utilities are therefore vulnerable to significant financial disruption during drought, and hydrologic financial risk can have an outsized impact on the long-term viability of the utility; indeed, credit rating agencies have noted that the ability to manage the financial impacts of drought is an important factor in determining a utility's creditworthiness (Chapman & Breeding, 2014; Moody's Investors Service, 2011, 2019). Tools such as reserve funds, financial hedging contracts, and lines of credit can be used to reduce the variability of net cash flows. This, in turn, can reduce an organization's likelihood of bankruptcy, improve its credit rating, and reduce its future borrowing costs (Bank & Wiesner, 2010; Pérez-González & Yun, 2013), in addition to helping risk-averse staff feel more comfortable (Bodnar, Giambona, Graham, & Harvey, 2019; Krause & Tse, 2016). Most utilities rely heavily on debt to finance infrastructure projects (Hughes & Leurig, 2013), so financial risk management is a key component of providing quality service at affordable rates.

Despite the critical role of financial risk management in water resources, decision support for practitioners in this area has remained limited. There is a long history of considering financial objectives such as expected revenues and costs in water resources systems analysis (e.g., see references in Labadie (2004); Macian-Sorribes and Pulido-Velazquez (2019); Yeh (1985)). However, fewer studies have explicitly accounted for variability in costs and revenues, or the financial risk management actions that an organization can take to combat this variability. Those that do have tended to propose static, non-adaptive management strategies. For example, modeling of financial reserves is not common in the water resources literature, and the limited examples tend to assume that the utility will contribute either a fixed amount or a fixed fraction of revenues to the reserve fund each year (Rehan, Knight, Unger, & Haas, 2013; Rehan, Unger, Knight, & Haas, 2015; Zeff, Kasprzyk, Herman, Reed, & Characklis, 2014). Similarly, there is a growing interest in using hydrology-based financial hedging contracts in applications such as hydropower (Foster, Kern, & Characklis, 2015; Hamilton, Characklis, & Reed, 2020; Meyer, Characklis, Brown, & Moody, 2016), water supply (Brown & Carriquiry, 2007; Maestro, Barnett, Coble, Garrido, & Bielza, 2016; Zeff & Characklis, 2013), and agriculture (Denaro, Castelletti, Giuliani, & Characklis, 2020; Mortensen & Block, 2018; Turvey, 2001), but researchers have generally assumed that the same contract is purchased each year, not allowing for risk management to be adjusted over time as conditions change.

However, financial researchers have demonstrated that adaptive, state-aware action is crucial to financial risk management (Bolton, Chen, & Wang, 2011; Disatnik, Duchin, & Schmidt, 2014; Froot, Scharfstein, & Stein, 1993; Rampini, Sufi, & Viswanathan, 2014). Just as a reservoir operator should consider current reservoir levels and expected future inflows when making release decisions, so should a financial risk manager consider the utility's current bank account balance and projected future revenues and costs when deciding whether to withdraw money from the bank, or whether to hedge its drought exposure using index contracts. A variety of optimization methods have been applied to financial problems such as investment portfolio selection (Markowitz, 1952; Mulvey, 2001; Pardalos, Sandström, & Zopounidis, 1994), asset-liability management (Kouwenberg & Zenios, 2008; Sodhi, 2005), and cash flow management (Baumol, 1952; da Costa Moraes, Nagano, & Sobreiro, 2015; Miller & Orr, 1966). As in water resources systems analysis, some researchers have attempted to provide more realistic decision support using multi-objective formulations (de Almeida-Filho, de Lima Silva, & Ferreira, 2020; Marqués, García, & Sánchez, 2020; Salas-Molina, Pla-Santamaria, & Rodriguez-Aguilar, 2018; Zopounidis, Galariotis, Doumpos, Sarri, & Andriosopoulos, 2015), model-free information (Sun, Fang, Wu, Lai, & Xu, 2011), heuristic solution methods (Aguilar-Rivera, Valenzuela-Rendón, & Rodríguez-Ortiz, 2015; da Costa Moraes & Nagano, 2013; Ponsich, Jaimes, & Coello Coello, 2013; Tapia & Coello Coello, 2007), and visual analytics (Flood, Lemieux, Varga, & William Wong, 2016; Savikhin, Lam, Fisher, & Ebert, 2011). Beyond the academic literature, the use of quantitative decision support tools by financial firms (e.g., banks, hedge funds, insurers) has proliferated in recent years, driven by growth in computing power, big data, algorithms, and visualization software (Fabozzi, Focardi, & Jonas, 2007; Rundo, Trenta, di Stallo, & Battiato, 2019; Zopounidis, Doumpos, & Niklis, 2018). However, these firms generally employ proprietary and highly problem-specific technologies that are not readily adoptable by organizations outside of the financial sector, such as water and power utilities, which nevertheless face significant financial risks.

This paper bridges the gap between reservoir control and financial risk management to show how computational tools developed for the former can be adapted to the latter. This research builds on prior work by the authors dealing with drought-related financial risk management by a hydropower producer. First, Hamilton et al. (2020) developed a hydro-financial simulation model that abstracts the hydroclimatology, hydropower generation, cash flows, and financial risk management of the Power Enterprise of the San Francisco Public Utilities Commission (SFPUC). The authors used this model to evaluate different static financial risk management portfolios within a Monte Carlo framework and search for optimal portfolios using an MOEA. In related work, Gupta, Hamilton, Reed, and Characklis (2020) introduced an adaptive EMODPS formulation of a simplified financial risk management problem, which was used to diagnostically benchmark if modern MOEAs are capable of addressing this new class of problem. The present study builds on these prior works by contributing the most detailed and actionable representation to date of how EMODPS can be used to craft operating policies that adapt to changing conditions over time when managing drought-related financial risk. The advantages of dynamic decision-making are demonstrated relative to a simplified static operating policy akin to those commonly applied to financial risk management in the water resources literature. This paper also demonstrates the value of higher-dimensional problem framings that explicitly account for decision-maker preferences with respect to the use of different management tools. Lastly, a framework is contributed for combining *a posteriori* visual analytics with information theoretic sensitivity analysis (ITSA) in order to help decision-makers better understand how complex, non-linear operating policies achieve their goals by adapting to real-time information when making decisions.

2 Study context

2.1 Study area

San Francisco Public Utilities Commission (SFPUC) owns and operates three reservoirs (Hetch Hetchy Reservoir, Cherry Lake, and Lake Eleanor) in the upper Tuolumne River basin in the Sierra Nevada mountains (Figure S1 in Supporting Information (SI)). These reservoirs deliver drinking water to much of the San Francisco Bay area, and en route, the water also provides hydroelectric power. SFPUC uses this hydropower to sell retail electricity at fixed rates to San Francisco International Airport, municipal buildings in San Francisco, and a number of other retail customer classes within the Bay area.

Irrigation districts along the Tuolumne River also have the right to buy surplus hydropower, when available, at a fixed rate. When hydropower production is in excess of retail and irrigation district demands, it is sold at floating market rates into the Western Systems Power Pool (hereafter "wholesale market"). On the other hand, when hydropower is insufficient to meet the demand from retail customers, SFPUC is obligated to purchase the remainder on the wholesale market. Although SFPUC provides both water supply and power supply, they are operated as independent entities from a financial perspective (San Francisco Public Utilities Commission, 2016), and the present work considers only the power supply enterprise.

2.2 Hydro-financial simulation model

This paper adopts the hydro-financial simulation model from Hamilton et al. (2020). The first component of the model is the stochastic engine, which is used to create a million-year synthetic record that can be used to drive the system. First, snow water equivalent depth (SWE) measurements for February 1 and April 1 (the months with the longest and most continuous datasets for the watershed) are randomly generated based on a copula model. Next, hydropower production is synthetically generated using piecewise linear models for each month conditioned on SWE, combined with an autoregressive model for residual noise. Third, monthly wholesale power prices are synthetically generated using a seasonal autoregressive moving average model. Lastly, monthly hydropower net revenues are calculated based on hydropower generation and power prices. Net revenues are defined as the total annual cash flow resulting from retail and wholesale hydropower sales, minus wholesale power purchases, minus the annual "fixed costs" (debt service payments, operations and maintenance, salaries, etc.) that must be paid each year. The synthetic records are found to closely match the historical record in terms of statistical properties, while providing a wider sampling of possible outcomes than can be found in the limited historical data. For more details on the methodology and validation of the stochastic engine, see Hamilton et al. (2020).

Three annual quantities are derived from this monthly synthetic dataset and used as stochastic drivers for the present study. Firstly, the SWE index (ε^S, in inches) is a weighted average of February and April SWE observations. The inflows to SFPUC's reservoirs are dominated by the seasonal dynamics of snow accumulation and melt, so SWE measurements taken upstream of the reservoirs in the late winter/early spring can be used to predict the magnitude of streamflows during the melt period in the late spring/early summer. A weighted average of February and April observations is found to improve correlation with annual hydropower production, relative to either month in isolation, by incorporating information about the timing of snowfall and melt (Hamilton et al., 2020). This correlation suggests that the index is a good candidate for financial hedging with index contracts (see below). The second stochastic driver is total hydropower net revenue over the water year (ε^R, in \$M). Lastly, the power price index (ε^P, in \$/MWh) is defined as the expected value of the generation-weighted average wholesale power price over the coming water year. This index takes advantage of autocorrelation in the market to predict how favorable the wholesale power prices will be for the utility's net hydropower revenues over the coming water year. Although the correlation is relatively low ($\rho = 0.35$, see SI Figure S2), the index still provides potentially valuable information for making decisions regarding financial risk, and is used as one of the inputs to the dynamic control policies (Section 3.1.2). More details on ε^P can be found in SI Section S1.

Absent any financial risk management, the utility will experience years in which costs outweigh revenues (i.e., net revenue is negative). This situation can be extremely disruptive because the utility risks defaulting on its obligations (e.g., debt service or operations and maintenance). The hydro-financial simulation model provides three tools which can be used to avoid such negative outcomes. Firstly, it can purchase a snowpack-based hedging contract called a capped Contract for Differences (CFD). The CFD (SI Figure S3) provides payouts to the utility in low-SWE years (below 24.7 inches), when it expects to have low hydropower and thus low revenue, in return for the utility making payments in high-SWE years (above 24.7 inches), when the utility expects to have abundant hydropower and surplus revenue. The negative correlation between hydropower revenue and CFD payout has been found to significantly reduce the volatility of the combined cash flow, suggesting its value as a financial risk management tool (Hamilton et al., 2020). The second risk management tool is a reserve fund, into which the utility can deposit surplus cash flows. This allows it to withdraw from the fund when hydropower revenues are insufficient to pay its bills. Lastly, the utility has a letter of credit with a bank, under which it can borrow money (i.e., issue short-term debt). The debt is paid back each year (with interest), and is assumed to take up the slack in situations where the other two tools fail to generate sufficient cash flows to avoid defaulting on the utility's obligations. Note that the short-term debt considered in this model is distinct from longer-term debt service obligations related to past bond offerings, typically associated with infrastructure investments, and which are assumed to be part of the "fixed costs" above.

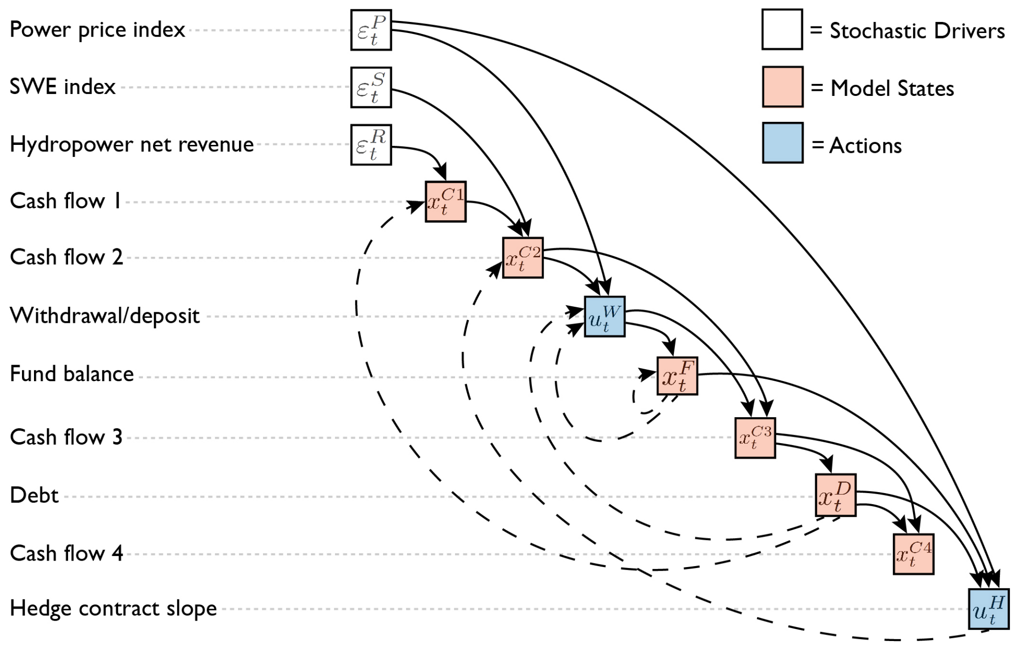

Figure 2. Annual sequence of operations in hydro-financial simulation model (moving from top left to bottom right). Solid (dashed) arrows represent the information flows from the current (previous) time step.

Figure 2 shows how these financial operations are abstracted in the hydro-financial simulation model (see Table 1 for a list of variable names, symbols, units, and constants). The sequence of operations occurs at the end of each water year, September 30, based on the stochastic outcomes that occur over the course of that water year, $\boldsymbol{\varepsilon}_t$. Two state-aware "actions" each year are governed by the control policy (to be described in Section 3.1): the amount of cash withdrawn from/deposited to the reserve fund (u_t^W, in \$M, where $u_t^W > 0$ represents a withdrawal and $u_t^W < 0$ represents a deposit), and the hedging contract slope (u_t^H, in \$M/inch of SWE). All other variables ("model states") are automatically updated according to the following rules:

$$x_t^{C1} = \varepsilon_t^R - r^D x_{t-1}^D \tag{1}$$

$$x_t^{C2} = x_t^{C1} + u_{t-1}^H h\left(\varepsilon_t^S\right) \tag{2}$$

$$x_t^F = r^F x_{t-1}^F - u_t^W \tag{3}$$

$$x_t^{C3} = x_t^{C2} + u_t^W \tag{4}$$

$$x_t^D = \max(-x_t^{C3}, 0) \tag{5}$$

$$x_t^{C4} = x_t^{C3} + x_t^D \tag{6}$$

where x_t^{C1}, x_t^{C2}, and x_t^{C3} are intermediate cash flows and x_t^{C4} is the final cash flow in year t; x_t^D and x_t^F are the short-term debt and reserve fund balance at the end of time step t; r^D and r^F are the annual real interest rates on debt and reserves; and $h\left(\varepsilon_t^S\right)$ is the CFD payout function (SI Figure S3). This function converts the stochastic SWE index value from the current year into a number of inches of SWE for which the utility will receive compensation (if $h\left(\varepsilon_t^S\right) > 0$) or owe payment (if $h\left(\varepsilon_t^S\right) < 0$). To get the utility's total payout received (or payment due), this output is multiplied by the CFD slope, u_{t-1}^H, as chosen by the control policy at the end of the previous year (Section 3.1). The reader is referred to Hamilton et al. (2020) for more details on construction of the CFD.

A full realization of the hydro-financial simulation model requires iterating this sequence for $T = 20$ years, subject to a randomly sampled $(T+1)$-year sequence of stochastic drivers. The multi-year simulation accounts for the path-dependent dynamics of the reserve fund and debt, as well as the autocorrelation within the stochastic power prices. The reserve fund and debt are assumed to be zero at $t = 0$ (in practice these values could be set based on circumstance). The hedging contract policy in year 0 (the slope to be used for the payout in year 1) is calculated using x_0^F, x_0^D, and ε_0^P.

3 Methods

Figure 3 shows how the stochastic engine and hydro-financial model are integrated into the broader framework of this study. The EMODPS methodology combines adaptive control rules, Monte Carlo ensemble simulation, and MOEA-driven policy search. The search produces a large population of candidate policies, which can be explored using optimal tradeoff analysis, many-objective visualization, and information theoretic sensitivity analysis. This framework is further described in what follows.

Table 1. Variables and constants for hydro-financial simulation model.

Variable	Symbol	Value	Units
Power price index	ε_t^P	-	\$/MWh
SWE index	ε_t^S	-	inches
Annual net revenue	ε_t^R	-	\$M
Cash flow 1	x_t^{C1}	-	\$M
Cash flow 2	x_t^{C2}	-	\$M
Withdrawal	u_t^W	-	\$M
Reserve fund balance	x_t^F	-	\$M
Cash flow 3	x_t^{C3}	-	\$M
Debt	x_t^D	-	\$M
Cash flow 4	x_t^{C4}	-	\$M
Hedge contract slope	u_t^H	-	\$M/inch
Mean net revenue before risk management	$\bar{R}$	10.99	\$M
Real discount rate	r^A	0.9615	-
Real interest rate on fund	r^F	0.9825	-
Real interest rate on debt	r^D	1.0100	-
Time horizon	T	20	years
Debt sustainability constraint	ϵ	0.05	\$M
Normalization for power price index	k^P	350	\$/MWh
Normalization for hedge contract slope	k^H	4	\$M/inch
Normalization for revenues & cash flows	k^R	250	\$M
Normalization for fund & debt	k^F	150	\$M

3.1 Control formulations

Within the hydro-financial simulation model, there are two important decisions that must be made each year: the hedging contract slope and the withdrawal from/deposit to the reserve fund. A control policy refers to a structured set of rules for making these two decisions each year. This study introduces two types of control: static (or open-loop) policies, which perform the same actions with each time step (Section 3.1.1), and dynamic (or closed-loop) policies, which adapt to changing conditions over time (Section 3.1.2).

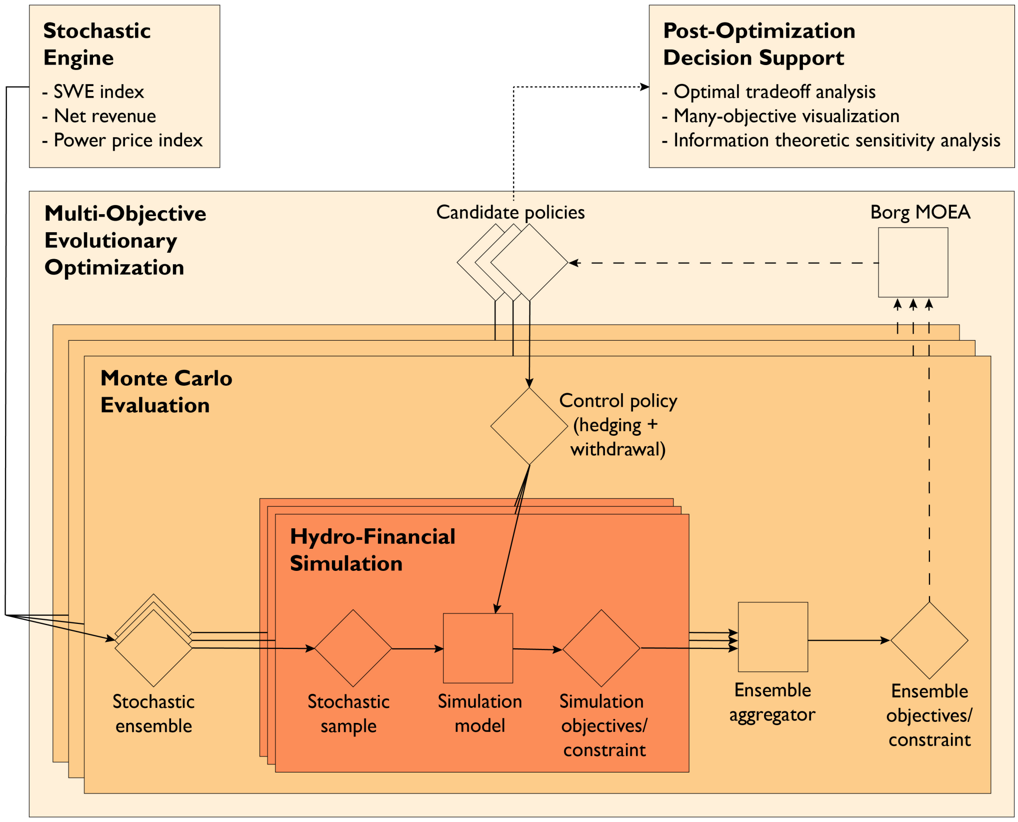

Figure 3. Schematic showing overall workflow for this study. Rectangles represent modules and diamonds represent inputs/outputs. Dashed arrows show the feedback process for the Borg MOEA, where objective and constraint values from prior control policy evaluations are used to generate new candidate policies for evaluation. The dotted arrow represents the final population output from the MOEA search, which is used as input to the post-optimization decision support.

Dynamic policies are considered state-aware because the decisions at each time step are conditioned on the current state of the model. Under both static and dynamic formulations, a policy is defined by a parameter vector which governs its operations. Multi-objective evolutionary optimization (Section 3.3) will be used to search for parameter vectors that perform well across four objectives related to the annualized cash flow, the risk of extreme debt levels, the probability of using hedging contracts, and the size of the reserve fund (Section 3.2).

3.1.1 Static policies

The static control formulation (adapted from Hamilton et al. (2020)) is given by:

$$\boldsymbol{\theta}_{stat} = [u^H, x^F_{max}] \tag{7}$$

where $\boldsymbol{\theta}_{stat}$ is the policy parameter vector and u^H and x^F_{max} are the two parameters to be optimized. u^H is the CFD slope, which is held fixed across all years in the simulation, while x^F_{max} is the maximum allowable reserve fund. Given x^F_{max}, the reserve fund operates according to the following simple rules: If the intermediate cash flow is negative ($x^{C2}_t < 0$), cash is withdrawn from the reserve fund to make up the deficit if possible. If $x^{C2}_t > 0$, the surplus is deposited into the fund, up until the fund has reached x^F_{max}. This policy is referred to as "static" because the CFD slope does not react to changing conditions (i.e., it is not state-aware). Although the withdrawal policy is quasi-state-aware via cash-balance constraints (money can neither be created nor destroyed), it is not truly dynamic in a meaningful sense (e.g., it cannot condition its reserve fund target on power price projections). Note that in Figure 2, the static formulation does not include the three input arrows into u^H_t, and only includes the two input arrows into u^W_t that relate to the cash balance constraints (x^{C2}_t and x^F_{t-1}).

3.1.2 Dynamic policies using Direct Policy Search (DPS)

The dynamic control formulation conditions the decision at each time step on the information available at that time. For a decision $u^{\mathcal{D}}_t$, with $\mathcal{D} \in \{W, H\}$ representing the withdrawal and hedging decisions, respectively:

$$u^{\mathcal{D}}_t = \mathcal{P}^{\mathcal{D}}(\boldsymbol{\mathcal{I}}^{\mathcal{D}}_{t'} | \boldsymbol{\theta}^{\mathcal{D}}_{dyn}) \tag{8}$$

where $\mathcal{P}^{\mathcal{D}}$ is the mathematical form of the policy for decision $\mathcal{D}$ (e.g., discrete policy table for SDP), $\boldsymbol{\theta}^{\mathcal{D}}_{dyn}$ is the vector of parameters to be optimized for the policy, and $\boldsymbol{\mathcal{I}}^{\mathcal{D}}_{t'}$ is the information upon which the decision is conditioned. This information can be any subset of the model states, actions, and stochastic drivers. The subscript t' on each element represents either the current (t) or previous ($t-1$) time step, based on the sequential nature of decisions (see Figure 2).

In DPS, $\mathcal{P}$ is assumed to be a family of parametric functions (Rosenstein & Barto, 2001). This approximation drastically reduces the number of decision variables in the search relative to SDP (Bertsekas, 2019; Powell, 2019). Many parametric function families are available (e.g., piecewise linear, polynomial, artificial neural network), but radial basis functions (RBFs) have been shown to be efficient universal approximators for DPS (Giuliani, Mason, Castelletti, Pianosi, & Soncini-Sessa, 2014). In this work, a sum of RBFs is paired with a constant shift parameter, along with an outer function that performs operations such as normalization and constraints. Equation 8 can be rewritten as:

$$u_t^{\mathcal{D}} = \phi^{\mathcal{D}} \left(a^{\mathcal{D}} + \sum_{m=1}^{M} w_m^{\mathcal{D}} \varphi_m \left(\boldsymbol{\mathcal{I}}_{t'}^{\mathcal{D}} \right) \right) \tag{9}$$

where $\phi^{\mathcal{D}}$ is the outer function, $a^{\mathcal{D}} \in [-1, 1]$ is a constant shift, and $w_m^{\mathcal{D}}$ is the weight given to the mth out of M total RBFs, φ_m. The weights must be chosen such that $\sum_{m=1}^{M} w_m^{\mathcal{D}} = 1$, and $w_m^{\mathcal{D}} \geq 0$ for all m. The RBF is defined

$$\varphi_m(\boldsymbol{\mathcal{I}}_{t'}^{\mathcal{D}}) = \exp \left(- \sum_{l=1}^{L} \frac{\left(\left[\boldsymbol{\mathcal{I}}_{t'}^{\mathcal{D}} \right]_l - c_{l,m} \right)^2}{(b_{l,m})^2} \right) \tag{10}$$

where $\left[\boldsymbol{\mathcal{I}}_{t'}^{\mathcal{D}} \right]_l$ is the lth out of L informational inputs, and $c_{l,m} \in [-1, 1]$ and $b_{l,m} \in (0, 1]$ are the center and radius, respectively, of the mth RBF in the direction of the lth input. The M RBFs are shared by the two decisions in the control policy.

The information vector for each decision includes the combination of state variables and external drivers that might be useful for making the decision:

$$\boldsymbol{\mathcal{I}}_{t'}^{W} = \left[r^F \tilde{x}_{t-1}^F, \quad r^D \tilde{x}_{t-1}^D, \quad \tilde{\varepsilon}_t^P, \quad \tilde{x}_t^{C2} \right] \tag{11}$$

$$\boldsymbol{\mathcal{I}}_{t'}^{H} = \left[\tilde{x}_t^F, \quad \tilde{x}_t^D, \quad \tilde{\varepsilon}_t^P \right] \tag{12}$$

where all tildes represent values that have been normalized to lie between 0 and 1, using the normalization constants in Table 1. Both decisions utilize information about the reserve fund balance and debt, but $u^{\mathcal{D}}$ uses last year's balance plus accumulated interest, while $u^{\mathcal{W}}$ uses the updated value from the present year (Figure 2). Both decisions also use the current power price index. Finally, the cash flow prior to withdrawal/deposit, x_t^{C2}, is used for $u^{\mathcal{W}}$ but not $u^{\mathcal{D}}$. Because the M RBFs are shared across the two decisions, $L = \max(L^W, L^H) = 4$.

The outer functions ϕ^W and ϕ^H (Equation 9) each consist of multiple nested functions performing specific operations. The more straightforward ϕ^H consists of a normalization function, ϕ^{HN}, and a constraint function, ϕ^{HC}. Let z_t be the argument to ϕ^H, the action prescribed by the constant shift and sum of radial basis functions in Equation 9 when H is substituted for $\mathcal{D}$. This equation can be decomposed as

$$u_t^H = \phi^H(z_t) = \phi^{HC} \left(\phi^{HN}(z_t) \right) \tag{13}$$

First, ϕ^{HN} scales the hedging contract slope to the proper scale, $[0, k^H]$ ($M/inch), where k^H is the hedging contract normalization constant in Table 1.

$$z'_t = \phi^{HN}(z_t) = k^H \max(\min(z_t, 1), 0) \tag{14}$$

Next, ϕ^{HC} constrains the contract slope to be greater than or equal to a constant threshold, $k^H d^H$, where the threshold parameter $d^H \in [0, 1]$ is included in the policy parameter vector to be optimized, along with a^H, $\mathbf{w}^H$, $\mathbf{c}$, and $\mathbf{b}$.

$$u^H_t = \phi^{HC}(z'_t) = \begin{cases} z'_t, & \text{if } z'_t \geq k^H d^H \\ 0, & \text{otherwise} \end{cases} \tag{15}$$

The outer function for the withdrawal decision, ϕ^W, consists of four nested operations. Let z_t now be the sum of the constant shift and RBFs in Equation 9 when W is substituted for $\mathcal{D}$. Then:

$$u^W_t = \phi^W(z_t) = \phi^{WCO}\left(\phi^{WCI}\left(\phi^{WW}\left(\phi^{WN}(z_t)\right)\right)\right) \tag{16}$$

where ϕ^{WCO}, ϕ^{WCI}, ϕ^{WW}, and ϕ^{WN} are the outer constraint, inner constraint, withdrawal transformation, and normalization functions. First, when designing the withdrawal policy, it was discovered that the EMODPS search produces better results when z_t is defined as the prescribed post-withdrawal cash flow rather than the withdrawal itself. For this reason, the normalization function, ϕ^{WN}, transforms z_t to the scale of $[-k^R, k^R]$ ($M), where k^R is the normalization constant for all revenues and cash flows in Table 1.

$$z'_t = \phi^{WN}(z_t) = k^R \max(\min(2z_t - 1, 1), -1) \tag{17}$$

The withdrawal transformation function, ϕ^{WN}, transforms z'_t from a cash flow into a withdrawal/deposit using the relationship between incoming and outgoing cash flow:

$$z''_t = \phi^{WW}(z'_t) = z'_t - x^{C2}_t \tag{18}$$

The inner constraint function, ϕ^{WCI}, ensures that the withdrawal/deposit is consistent with cash-balance equations:

$$z'''_t = \phi^{WCI}(z''_t) = \begin{cases} \min\left(z''_t, \quad r^F x^F_{t-1}\right), & \text{if } z''_t >= 0 \\ \max\left(z''_t, \quad -max\left(x^{C2}_t, 0\right)\right), & \text{otherwise} \end{cases} \tag{19}$$

The first condition ensures that a withdrawal ($z_t'' > 0$) cannot be larger than the balance in the reserve fund. The second case dictates that a deposit ($z_t'' < 0$) is only allowed when the available cash flow x_t^{C2} is positive, and that the deposit cannot be larger in magnitude than this cash flow.

Lastly, the outer constraint, ϕ^{WCO}, ensures that the reserve fund balance (after withdrawal/deposit) cannot be larger than a constant threshold, $k^F d^W$, where k^F (\$M) is the normalization constant used for the reserve fund and debt in Table 1, and $d^W \in [0,1]$ is another decision variable to be optimized.

$$u_t^W = \phi^{WCO}(z_t''') = \begin{cases} r^F x_{t-1}^F - k^F d^W, & \text{if } \left(r^F x_{t-1}^F - z_t'''\right) > k^F d^W \\ z_t''', & \text{otherwise} \end{cases} \tag{20}$$

This threshold sets the maximum allowable reserve fund size, equivalent to x_{max}^F in the static formulation.

Equations 8-20 constitute the full dynamic control policy. The parameter vector to be optimized for each decision $\mathcal{D} \in \{W, H\}$ is

$$\boldsymbol{\theta}_{dyn}^{\mathcal{D}} = [a^{\mathcal{D}}, \quad d^{\mathcal{D}}, \quad \mathbf{w}^{\mathcal{D}}, \quad \mathbf{c}, \quad \mathbf{b}] \tag{21}$$

where $\mathbf{w}^{\mathcal{D}} = \left[w_0^{\mathcal{D}}, ..., w_M^{\mathcal{D}}\right]$, $\mathbf{c} = [c_{0,0}, ..., c_{L,M}]$, and $\mathbf{b} = [b_{0,0}, ..., b_{L,M}]$. The total parameter vector to be optimized, $\boldsymbol{\theta}_{dyn}$, is the set of unique parameters,

$$\boldsymbol{\theta}_{dyn} = [a^W, \quad a^H, \quad d^W, \quad d^H, \quad \mathbf{w}^W, \quad \mathbf{w}^H, \quad \mathbf{c}, \quad \mathbf{b}] \tag{22}$$

3.2 Objective formulations

This study uses "noisy" objective formulations to account for the uncertainty of outcomes under the stochastic drivers. Each candidate policy is evaluated using a Monte Carlo ensemble of N realizations, each representing one possible trajectory of the hydro-financial system under a T-year sample of the stochastic drivers. To convert an ensemble of time series into a scalar performance metric requires both a time aggregation step (e.g., taking the maximum debt over a T-year realization) and a noise filtering step (e.g., taking the 95th percentile over N realizations in the ensemble). Four objectives are considered in this study, each defined as the maximization or minimization of a particular performance metric.

The first objective is to maximize the expected annualized cash flow, J^{cash}, a measure of "average" cash flows. A high value represents a low-cost risk management policy. Although public utilities are not strictly profit-maximizing firms, they nonetheless aim to maintain sufficient cash flows to keep customer rates low and/or invest in new infrastructure, and J^{cash} is used as a proxy for this type of financial health.

$$J^{cash}\left(x^{C4}_{t\in(1,\ldots,T)}, x^F_T, x^D_T\right) = E_{\boldsymbol{\varepsilon}}\left[ANN_t\left(x^{C4}_{t\in(1,\ldots,T)}, x^F_T, x^D_T\right)\right] \tag{23}$$

where x^{C4}_t is the final cash flow for year t; x^F_T and x^D_T are the reserve fund balance and debt at the end of the simulation; $E_{\boldsymbol{\varepsilon}}$ is the expectation over the stochastic drivers (approximated by the mean of N Monte Carlo samples); and ANN_t is the annualization operator:

$$ANN_t\left(x^{C4}_{t\in(1,\ldots,T)}, x^F_T, x^D_T\right) = \frac{1}{\sum_{t=1}^{T}(r^A)^t}\left(\sum_{t=1}^{T}\left((r^A)^t x^{C4}_t\right) + (r^A)^{T+1}\left(r^F x^F_T - r^D x^D_T\right)\right) \tag{24}$$

where where r^A is the real discount rate and r^F and r^D are the real interest rates on reserves and debt (Table 1). ANN_t sums the net present value (NPV) of all discounted cash flows over T years, plus the NPV of the reserve fund and debt in year T, and divides this sum by a normalization factor. The normalized value represents the constant cash flow, or annuity, that is equivalent in terms of NPV to the variable cash flow. On the whole, annualization allows for a fair comparison, accounting for the time value of money, between cash flow time series resulting from different management strategies.

The second objective is to minimize J^{debt}, the 95th percentile of maximum debt. This is a measure of the short-term debt load that would be needed to meet fixed costs in an extremely bad year (or sequence of years). This performance metric is used as a proxy for "risk", and a decision-maker would want to minimize this quantity in order to avoid compromising the utility's credit rating, increasing future borrowing costs, and/or risking bankruptcy.

$$J^{debt}\left(x^D_{t\in(1,\ldots,T)}\right) = Q95_{\boldsymbol{\varepsilon}}\left[\max_{t\in(1,\ldots,T)}\left[x^D_t\right]\right] \tag{25}$$

where the *max* operator takes the maximum debt over a T-year realization, and the $Q95$ operator takes the 95th percentile over the Monte Carlo ensemble.

These first two objectives, adopted from Hamilton et al. (2020), are representative of the risk/return tradeoff analysis that is common in financial applications (Hull, 2009; Markowitz, 1952). However, financial researchers have found that higher-dimensional problem framings can more accurately represent managers' behavior in the empirical data (Spronk, Steuer, & Zopounidis, 2005; Zopounidis et al., 2015). For example, in addition to maximizing return and minimizing risk, an investment portfolio manager might want to minimize the number of unique securities held because this limits the associated paperwork, transactions fees, etc. Similarly, in workshops designed to help water utilities integrate MOEAs into their water portfolio planning processes, Smith et al. (2019) have found that managers often weigh the decision levers (e.g., whether a new reservoir must be built) alongside more traditional measures of portfolio performance (e.g., supply reliability) when deciding which portfolio to choose. This represents an expansion of the objective space in practice, and reflects decision-makers' expert knowledge of the tradeoffs associated with various management tools. Bringing together these lines of research, a utility manager would be expected to balance tradeoffs associated with different financial risk management tools in addition to performance metrics like risk and return (Bank & Wiesner, 2010; Hughes et al., 2014). Two additional objectives are now introduced in order to explore the impact of such tradeoffs.

The third objective is to minimize J^{hedge}, the expected hedging frequency.

$$J^{hedge}\left(u^H_{t\in(0,\ldots,T-1)}\right) = E_{\boldsymbol{\varepsilon}}\left[\max_{t\in(0,\ldots,T-1)}\left[\mathbf{1}_{u^H_t>0}\right]\right] \tag{26}$$

where the indicator function $\mathbf{1}_{u^H_t>0}$ returns a 1 if the hedging contract slope is non-zero, and a 0 otherwise. This metric represents the likelihood that the utility will enter into at least one hedging contract over the course of 20 years. Note that each hedging contract does have an annual cost, a "loading" applied by the contract seller that makes the expected payout of h (SI Figure S3) negative (Hamilton et al., 2020). However, this cost is already accounted for by J^{cash}, and does not need to be double-counted. J^{hedge}, rather, relates to the significant extra costs (in time, personnel, and/or money) of having to set up the first hedging contract within a realization, assuming that this start-up cost will be significantly diminished in subsequent contract purchases. Moreover, this objective can be taken to represent the general discomfort that a utility manager may have with financial hedging contracts due to their novelty and perceived complexity or opacity (Bank & Wiesner, 2010).

The last objective is to minimize J^{fund}, the expected maximum reserve fund balance.

$$J^{fund}\left(x^F_{t\in(1,\ldots,T)}\right) = E_{\boldsymbol{\varepsilon}}\left[\max_{t\in(1,\ldots,T)}\left[x^F_t\right]\right] \tag{27}$$

This metric represents the expected value of the largest reserve fund used in a T-year realization, which a utility manager may want to minimize in order to avoid attracting regulatory scrutiny over holding large liquid reserves (Hughes et al., 2014).

Finally, a "debt sustainability" constraint ensures that feasible policies do not allow debt to grow unchecked over time (on average), which would likely lead to a credit downgrade in practice:

$$E_{\boldsymbol{\epsilon}}\left[x_T^D - x_{T-1}^D\right] < \epsilon \tag{28}$$

where ϵ is a small constant (Table 1). This "noisy" constraint is calculated from the entire Monte Carlo ensemble; there is no constraint on debt use in individual extreme realizations.

3.3 Multi-objective evolutionary optimization of control policies

As described in Sections 1 and 3.1.2, DPS has a number of advantages relative to traditional methods such as SDP, especially when combined with non-linear approximating networks such as RBFs. However, RBF parameterization can result in a highly nonlinear and non-convex search space that is difficult to traverse with gradient-based methods, especially when combined with noisy multi-objective formulations (Giuliani & Castelletti, 2016; Giuliani, Mason, et al., 2014; Giuliani et al., 2018). These problems are better handled by MOEAs, which use evolution-inspired strategies (e.g., selection, mating, mutation) to iteratively improve a population of solutions competing on multiple objectives (Coello Coello, Lamont, & Van Veldhuizen, 2007). Population-based methods can approximate the entire Pareto set in a single run, rather than rerunning many single-objective optimizations, making them quite efficient on many-objective problems. Additionally, these heuristic approaches require no information on the topology of a problem and are well-adapted to the types of nonlinear, non-convex, high-dimensional, and stochastic problems that are common in both water resources (Maier et al., 2014; Nicklow et al., 2010; Reed, Hadka, Herman, Kasprzyk, & Kollat, 2013) and finance (Ponsich et al., 2013; Tapia & Coello Coello, 2007).

This study employs the Borg Multiobjective Evolutionary Algorithm (MOEA) (Hadka & Reed, 2013), which has been particularly successful across a range of difficult problems in water resources (Gupta et al., 2020; Hadka & Reed, 2012; Reed et al., 2013; Zatarain Salazar, Reed, Herman, Giuliani, & Castelletti, 2016) and engineering design (Singh et al., 2020;

Woodruff, Reed, & Simpson, 2013). The Borg MOEA includes novel components such as adaptive search operator selection, adaptive population sizing, stagnation detection via epsilon-progress, and epsilon-dominance archiving. Its self-adaptive nature makes the Borg MOEA highly controllable (Hadka & Reed, 2013; Reed et al., 2013), and the master-worker parallel variant used in this study is scalable on high-performance computing infrastructure (Giuliani et al., 2018; Zatarain Salazar et al., 2017).

3.4 Information theoretic sensitivity analysis

A sensitivity analysis (SA) is an evaluation of the effects of a model's input factors on its output factors, and a wide range of methods are available to suit different purposes. According to the taxonomy of SA introduced by Pianosi et al. (2016), the method that follows would be considered a quantitative, global, "all-at-a-time" SA, based on simulation model output. This SA is used to explore how different policies adapt their actions to changing conditions; more specifically, it will probe the sensitivity of the prescribed hedging and withdrawal decisions (Equation 8) to changing informational inputs (Equations 11-12). This type of analysis can help to "open the black box" of control policies, helping decision-makers better understand how different policies respond to changing information (Quinn et al., 2019).

However, commonly-used variance-based methods, which decompose the variance of an output variable into contributions from covariance with different input variables, are inappropriate in the proposed context. First, the policies described by Equations 9-20 are highly non-linear and discontinuous, so that variance and covariance are inappropriate measures of variability and relationship. Secondly, most variance decomposition methods assume independence between the input variables, and can lead to misleading results when this independence is violated (Borgonovo, 2007; Borgonovo, Castaings, & Tarantola, 2011). This is especially problematic in the current context because most Pareto-optimal solutions will impose the following relationship between the reserve fund and debt: if one is large, the other is usually zero. For these reasons, moment-independent global SA methods, such as entropy-based SA (Auder & Iooss, 2009; Krzykacz-Hausmann, 2001), are preferred. Hejazi, Cai, and Ruddell (2008) use ITSA to study the impact of hydrologic information on historical release decisions made by reservoir operators under different conditions. A similar approach is adopted here to study how different policies along the Pareto front use model state information to make decisions.

Shannon entropy (Shannon, 1948) quantifies how much information is needed, on average, to describe a random variable. Consider $u^{\mathcal{D}}$, $\mathcal{D} \in \{W, H\}$, the two policy-prescribed actions. $u^{\mathcal{D}}$ is a function of the information vector, $\boldsymbol{\mathcal{I}}^{\mathcal{D}}$, which varies stochastically through time and across Monte Carlo realizations. As such, both the information vector and the prescribed action can be considered random variables, $\mathbf{I}^{D}$ and $U^{\mathcal{D}}$. The entropy of the action is:

$$H(U^{\mathcal{D}}) = -\sum_{u^{\mathcal{D}} \in \upsilon^{\mathcal{D}}} p(u^{\mathcal{D}}) \log_2 p(u^{\mathcal{D}}) \tag{29}$$

where $p(u^{\mathcal{D}})$ is the probability mass function (PMF) after discretizing the outcome to a discrete domain, $\upsilon^{\mathcal{D}}$. The entropy (in bits when written with a base-2 logarithm) can be thought of as a moment-free measure of uncertainty, or dispersion, in the probability distribution of a random variable. A variable whose outcome is known deterministically has zero entropy, while a uniformly distributed variable is the most uncertain and has the largest possible entropy. Although a continuous variant of entropy based on Kullback-Leibler divergence can also be used for SA (Auder & Iooss, 2009; Liu, Chen, & Sudjianto, 2006; Pappenberger, Beven, Ratto, & Matgen, 2008), the discrete version is more straightforward when the random variable's distribution is unknown.

The mutual information between two random variables measures the average reduction in the entropy of one variable when the other variable's outcome is known:

$$\begin{aligned} MI(\mathbf{I}_i^{\mathcal{D}}, U^{\mathcal{D}}) &= H(U^{\mathcal{D}}) - H(U^{\mathcal{D}}|\mathbf{I}_i^{\mathcal{D}}) && (30) \\ &= -\sum_{\boldsymbol{\mathcal{I}}_i^{\mathcal{D}} \in \boldsymbol{\iota}_i^{\mathcal{D}}} \sum_{u^{\mathcal{D}} \in \upsilon^{\mathcal{D}}} p(\boldsymbol{\mathcal{I}}_i^{\mathcal{D}}, u^{\mathcal{D}}) \log_2 \frac{p(\boldsymbol{\mathcal{I}}_i^{\mathcal{D}}, u^{\mathcal{D}})}{p(\boldsymbol{\mathcal{I}}_i^{\mathcal{D}}) p(u^{\mathcal{D}})} && (31) \end{aligned}$$

where $\mathbf{I}_i^{\mathcal{D}}$ is the random variable for the ith informational input (e.g., reserve fund balance or power price index), $H(U^{\mathcal{D}}|\mathbf{I}_i^{\mathcal{D}})$ is the entropy of the action conditional on the input, $p(\boldsymbol{\mathcal{I}}_i^{\mathcal{D}})$ is the PMF for the input on the discrete domain $\boldsymbol{\iota}_i^{\mathcal{D}}$, and $p(\boldsymbol{\mathcal{I}}_i^{\mathcal{D}}, u^{\mathcal{D}})$ is the joint PMF on the discrete domain $\boldsymbol{\iota}_i^{\mathcal{D}} \times \upsilon^{\mathcal{D}}$. This mutual information is a measure how much information the outcome of one random variable contains about the outcome of the other: how much does knowledge of a particular informational input reduce the uncertainty in the prescribed action?

Finally, the ITSA index is defined by dividing the mutual information by the entropy of the prescribed action:

$$\eta_i^{\mathcal{D}} = \frac{MI(\mathbf{I}_i^{\mathcal{D}}, U^{\mathcal{D}})}{H(U^{\mathcal{D}})} \tag{32}$$

where $\eta_i^{\mathcal{D}}$ is the sensitivity index for the ith input for decision $\mathcal{D}$. This index varies between 0 and 1; $\eta_i^{\mathcal{D}} = 0$ implies that $\mathbf{I}_i^{\mathcal{D}}$ and $U^{\mathcal{D}}$ are independent random variables, while $\eta_i^{\mathcal{D}} = 1$ implies perfect dependence (knowledge of $\boldsymbol{\mathcal{I}}_i^{\mathcal{D}}$ gives us perfect knowledge of $u^{\mathcal{D}}$).

4 Computational experiments

4.1 Problem formulations

This study considers both the static and dynamic control formulations, each of which has its own parameter vector to be optimized. The static parameter vector ($\boldsymbol{\theta}_{stat}$, Equation 7) has two elements to be optimized. The dynamic parameter vector, ($\boldsymbol{\theta}_{dyn}$, Equation 22) has $4 + 2M + 2ML$ elements, where $L = 4$ is the number of informational inputs, and M is the number of RBFs in the policy. With $M = 2$ RBFs (see next section), $\boldsymbol{\theta}_{dyn}$ contains 24 elements to be optimized.

For each control formulation, both two-objective and four-objective problems are considered. The two-objective problem can be written:

$$\boldsymbol{\theta}^* = \arg\min_{\boldsymbol{\theta}} \left[-J^{cash}(\boldsymbol{\theta}), \quad J^{debt}(\boldsymbol{\theta}) \right] \tag{33}$$

while the four-objective problem can be written:

$$\boldsymbol{\theta}^* = \arg\min_{\boldsymbol{\theta}} \left[-J^{cash}(\boldsymbol{\theta}), \quad J^{debt}(\boldsymbol{\theta}), \quad J^{hedge}(\boldsymbol{\theta}), \quad J^{fund}(\boldsymbol{\theta}) \right] \tag{34}$$

For both problems, the feasible solution space is restricted to solutions satisfying the sustainable debt constraint (Equation 28). The two-objective problem is the same as that used by Hamilton et al. (2020), allowing for a direct comparison, while the four-objective problem provides more nuanced insight into risk management tradeoffs.

4.2 MOEA experiments

An ensemble of $N = 50,000$ realizations is run for each function evaluation, balancing computational demand against the need to minimize sampling error in the noisy objective/constraint evaluations (see discussions in Kasprzyk et al. (2012); Quinn, Reed, Giuliani, and Castelletti (2017); Zatarain Salazar et al. (2017)). In order to select the appropriate number of RBFs, the dynamic 4-objective formulation is repeated with 1, 2, 3, 4, 8, and 12 RBFs. Due to the inherent stochasticity of evolutionary algorithms, each optimization is repeated with 10 different random seeds. Each seed is run for 150,000 function evaluations (candidate policy trials). Final populations are assessed in terms of hypervolume, additive epsilon indicator, and generational distance (SI Figure S4), three common metrics for assessing convergence, consistency, and diversity of multi-objective solution sets (Coello Coello et al., 2007; Hadka & Reed, 2012; Reed et al., 2013). Results are found to be relatively insensitive to the number of RBFs used in the dynamic control policies, but $M = 2$ RBFs is chosen due to the robust performance across seeds. Next, 20 additional seeds are run for the dynamic 4-objective formulation with $M = 2$, and 30 seeds each are also run for the dynamic 2-objective, static 2-objective, and static 4-objective formulations. The best known Pareto approximate set for each formulation is the set of non-dominated solutions from across the 30 seeds. After using the same 50,000-member ensemble of 20-year simulations for all formulations/seeds in the initial optimization, each solution in the final Pareto approximate set for each formulation is rerun on a separate 50,000-member ensemble, for which results are reported. Important parameter values for the optimization can be found in SI Table S1; all other Borg MOEA parameters besides those listed are set to the default values (Hadka & Reed, 2013; Reed et al., 2013).

4.3 Information theoretic sensitivity analysis parameters

ITSA indices for each specific operating policy are calculated using a 50,000-member ensemble of 20-year simulations, yielding 1,000,000 realizations of $\boldsymbol{\mathcal{I}}_i^{\mathcal{D}}$ and $u^{\mathcal{D}}$. Each component is discretized into 50 bins in order to calculate the marginal and joint probability mass functions (Equations 29, 31). This process is repeated for each control policy in the Pareto set, yielding separate ITSA indices for each.

5 Results and discussion

5.1 Static vs. dynamic financial risk management

Figure 4 shows the resulting Pareto approximate sets from the 2-objective optimization problem (Equation 33), under both static and dynamic control formulations. Each point represents a different financial risk management policy. The ideal performance, denoted by a black star, would be achieved with a cash flow metric (J^{cash}) of \$10.99M (the average net revenue in the absence of any financial risk management) and a debt metric (J^{debt}) of zero. However, this is not possible due to the strong tradeoff between "risk" and "return" that is standard in financial risk applications: in order to achieve higher expected cash flows, the utility must forego costly risk management actions and therefore risk more extreme debt burdens in less favorable realizations. As discussed in Section 3.2, large short-term debt in our model can be viewed as a proxy for larger financial disruptions such as credit rating downgrades or bankruptcy in practice. Decision-makers will have to balance this tradeoff when selecting a particular policy for the utility to use, based on risk aversion, access to credit, and other organizational factors.

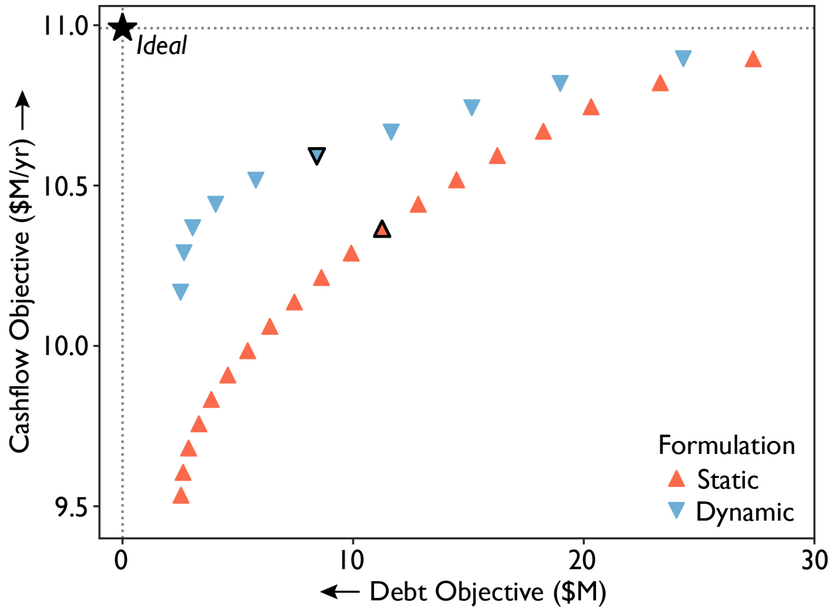

Figure 4. Comparison of 2-objective Pareto approximate sets under static and dynamic control formulations. The best compromise policy from each formulation is outlined in black and described in Table 2.

However, decision-makers can drastically reduce the risk management tradeoff by using adaptive operating rules that respond to changing conditions. The Pareto approximate set from the dynamic EMODPS control formulation is found to dominate the Pareto approximate set from the static formulation, suggesting that one can improve on both the cash flow and debt objectives simultaneously. For example, consider the two example policies outlined in black in Figure 4 and listed in Rows 1-2 in Table 2. These are chosen as the "best compromise" policies near the centers of their respective Pareto approximate sets (as selected using the TOPSIS method with equal weights on each objective (Behzadian, Khanmohammadi Otaghsara, Yazdani, & Ignatius, 2012; Roszkowska, 2011)). The dynamic policy is found to reduce J^{debt} by \$2.83M, or 25.1%, relative to the static policy. At the same time, it increases J^{cash} by \$0.23M, representing a 36.1% reduction in risk management cost. This dual improvement highlights the value of dynamic financial risk management: the utility can improve on both objectives simultaneously without requiring any investment in its infrastructure or changes to its physical operations. All that is required is to switch to a more dynamic financial risk management policy.

Table 2. Performance of six example policies referenced throughout the results sections. Rows 1 and 2 represent the best compromise policies from the static and dynamic control formulations, respectively, under the 2-objective optimization problem (Section 5.1). Row 3 represents the best compromise policy from the 4-objective optimization problem and the dynamic control formulation, after brushing with *a posteriori* constraints (Section 5.2). Rows 4-6 represent policies that are highly sensitive to information about the reserve fund balance, debt, and power price index, respectively (Section 5.3).

Row	Figure	J^{cash} (\$M/yr)	J^{debt} (\$M)	J^{hedge} (unitless)	J^{fund} (\$M)	Fund Sensitivity	Debt Sensitivity	Power Sensitivity
1	4 red	10.37	11.25	1.00	16.11	–	–	–
2	4 blue	10.59	8.42	1.00	19.31	0.74	0.11	0.12
3	8	10.75	15.90	0.77	12.01	0.36	0.72	0.01
4	9a	10.20	3.22	1.00	24.55	0.93	0.12	0.00
5	9b	10.71	15.72	0.40	16.83	0.44	0.96	0.01
6	9c	9.84	8.96	1.00	1.53	0.02	0.03	0.72

The dynamic formulation allows the utility to take different sequences of actions under different stochastic realizations, using parameterized control rules that allow for the actions taken at any particular time to be better tailored to the current state of the system. To elucidate the differences between static and dynamic financial risk management, the two best compromise policies are simulated under two different 20-year realizations from the synthetic record: an unusually wet period and an unusually dry period (Figure 5). Differences in SWE (5a) lead to drastic differences in hydropower generation (5b) and net revenues (5d) under the two realizations, and the dry scenario experiences lengthy periods of drought-related cash flow deficits. The two scenarios also yield very different responses in terms of the hedging policy (5e & 5i), reserve fund balance (5f & 5j), debt (5g & 5k), and final cash flow (5h & 5l). In the wet scenario, the reserve funds fill up quickly and stay nearly full. Neither policy requires any significant debt, and final cash flows are generally positive and rather large. In the dry scenario, the reserve funds fluctuate up and down, including two periods in which they reach zero. During these periods, significant debt is required to overcome further cash flow deficits. The final cash flows are close to zero throughout the dry simulation, as both policies struggle to fill their reserve funds.

With respect to the hedging contract, the static policy uses the same contract each year in both the wet and dry scenarios, with a payout slope of \$0.32M/inch. The dynamic policy, on the other hand, adjusts its contract slope from year to year. In the wet scenario, it opts not to hedge at all after year 0, while in the dry scenario, it fluctuates between \$0 and \$0.85M/inch. Comparing the hedging slope dynamics to the other model state variables suggests that this policy opts to hedge only when the reserve fund balance is low and/or when debt is non-zero. This strategy allows the dynamic policy to achieve higher cash flows than the static policy in wet scenarios (Sub-Figure 5h), by foregoing the cost of hedging contracts when the utility already has sufficient protection from a large reserve fund. On the other hand, when the reserve is empty and/or there is outstanding debt (presumably after a very dry year or sequence of years), the utility purchases large hedging contracts in order to increase its financial risk coverage and thus reduce the risk of extreme debt levels (Sub-Figure 5k). This adaptivity allows the dynamic policy to improve on both the cash flow objective and the debt objective simultaneously, compared to the static policy. As will be seen in Section 5.3, there are a multiplicity of ways that utilities can adapt to changing conditions to meet their goals.

5.2 Many-objective decision-making

As discussed in Section 3.2, a decision-maker choosing a financial risk management policy may actually consider other factors beyond risk (J^{debt}) and return (J^{cash}). For example, the utility might also worry about the size of the reserve fund needed to enact a particular policy (J^{fund}), or the likelihood of needing to develop and integrate a complicated hedging program (J^{hedge}). Such decision-makers are likely to find that none of the solutions found under the 2-objective problem (Figure 4) can meet their needs. The 2-objective problem cannot adequately represent important management tradeoffs

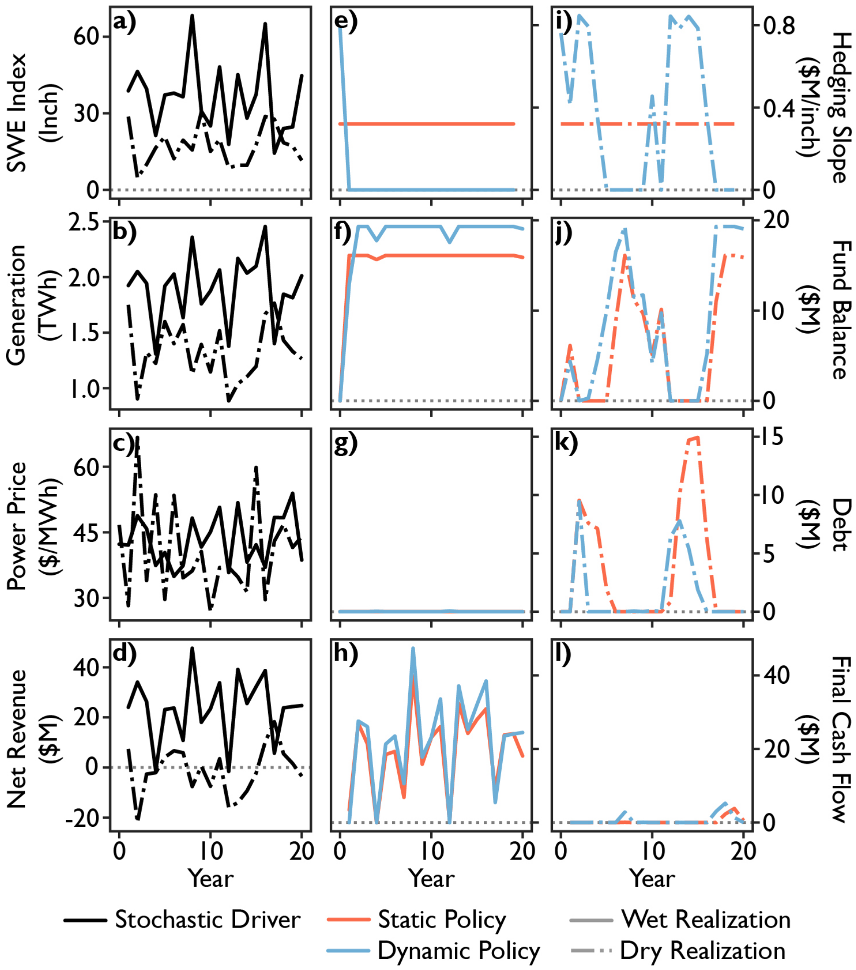

Figure 5. Trajectories for hydro-financial simulation model, over both wet and dry 20-year realizations, for the example static and dynamic policies shown in Figure 4 and Rows 1-2 of Table 2. Sub-Figures show (a) SWE index; (b) hydropower generation; (c) wholesale power price; (d) net hydropower revenue; (e & i) hedging slope action; (f & j) fund balance; (g & k) debt; and (h & l) final annual cash flow. Middle column (e-h) shares its y-axis with the right-hand column (i-l).

because it does not account for decision-maker preferences with respect to the use of different risk management tools. For this reason, J^{hedge} and J^{fund} can be explicitly included in the optimization using the 4-objective problem (Equation 34).

Both the static and dynamic formulations produce much larger Pareto approximate sets in this higher-dimensional problem (Figure 6), representing the more complex set of tradeoffs across the four objectives. The dynamic Pareto approximate set is found to generally outperform the static Pareto approximate set, especially in terms of the over-

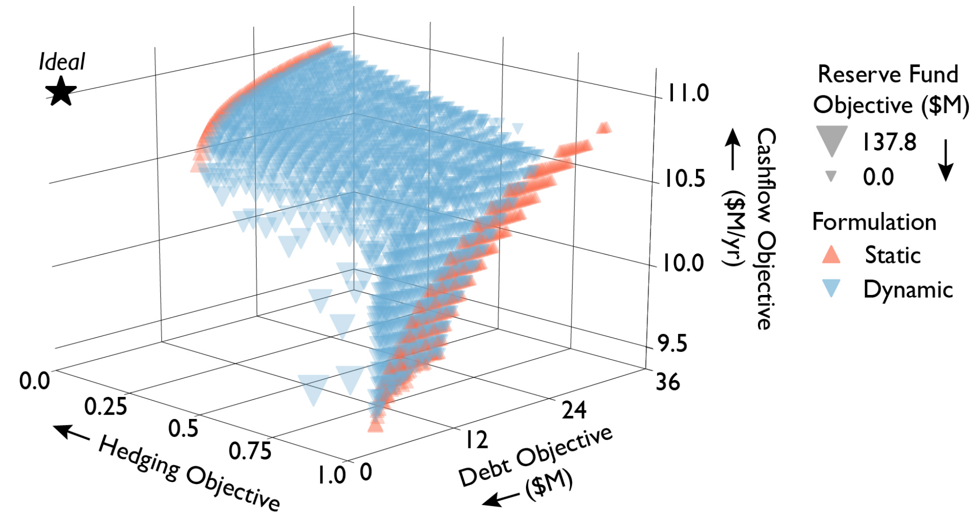

Figure 6. Comparison of 4-objective Pareto approximate sets under static and dynamic control formulations.

all diversity of solutions. For the static formulation, where the hedging contract slope is fixed, J^{hedge} must be equal to 1 or 0. The dynamic formulation, on the other hand, is able to find policies with J^{hedge} spanning the entire range from 0 to 1. Note that J^{hedge} is defined as the fraction of 20-year realizations that contain any hedging, not the fraction of years which hedge (see Equation 26). Thus, intermediate values between 0 and 1 represent solutions that are unlikely to hedge in any given year, but maintain the option to do so under particularly problematic circumstances. This valuable optionality is only possible with a dynamic control strategy. Additionally, the dynamic solution set occupies a much larger region within the ridge where $J^{hedge} = 1$. These policies outperform the nearest static policies with respect to J^{cash} and J^{debt}, but may require the use of larger reserve funds. Because the dynamic control method produces a much more complete and continuous Pareto approximate set, it allows decision-makers to find control policies that more precisely match their preferences.

A major benefit of solving the larger-dimensional problem is that the solution set will already contain all of the tradeoffs for all possible lower-dimensional problems (di Pierro, Khu, & Savić, 2007). In the present context, the 4-objective Pareto front will include within it the Pareto fronts for the four 3-objective problems, six 2-objective problems, and four 1-objective problems that are embedded within the 4-objective problem (Figure 7). In Sub-Figure 7a, the blue triangles show the subset of the 4-objective Pareto approximate set that is non-dominated with respect to the original two objectives, J^{cash} and J^{debt}. When compared to the original 2-objective solutions (Figure 4), the 4-objective policies are very similar with respect to the first two objectives. However, they can achieve improvements with respect to the two new objectives (see SI Figure S5). In other words, it is possible to improve J^{fund} and/or J^{hedge} with no penalty in J^{cash} or J^{debt}, but they must be included in the optimization explicitly to realize this benefit.

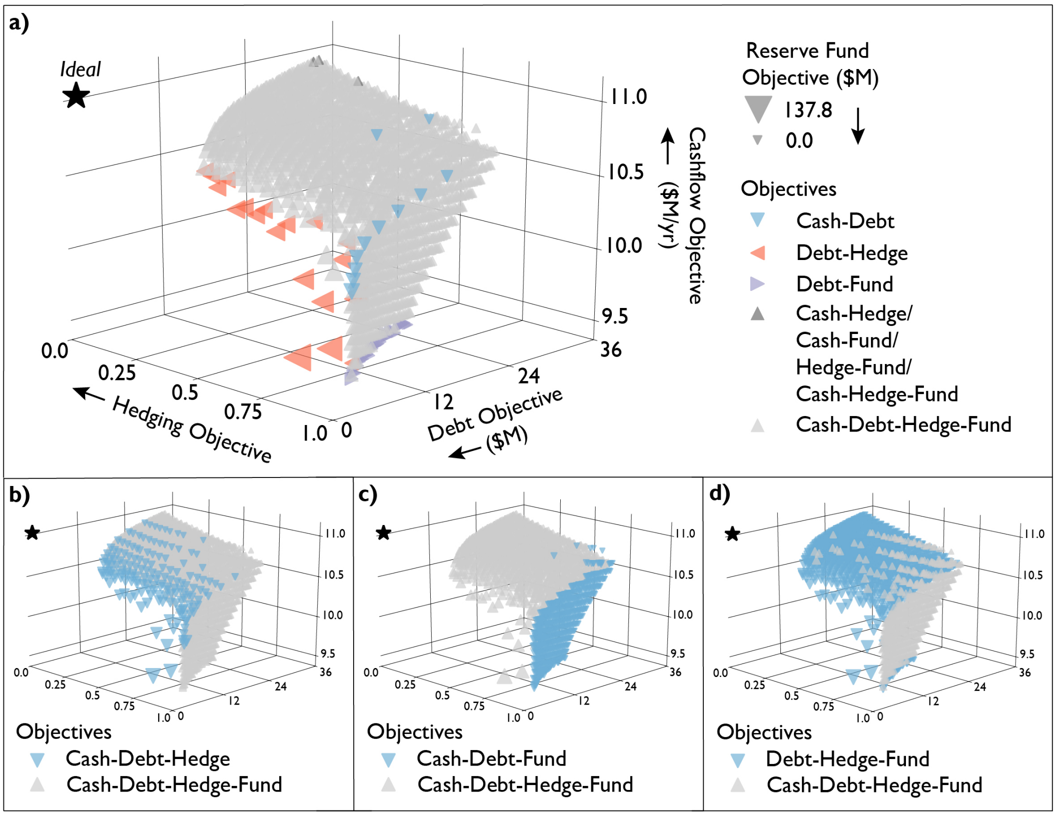

Figure 7. Visualization of Pareto approximate sets for different sub-problems. Colored points represent solutions that are non-dominated with respect to a particular sub-problem; for example, orange points in sub-figure (a) represent solutions that are non-dominated with respect to J^{debt} and J^{hedge}. Light grey points in all sub-figures represent solutions from the 4-objective problem that are not captured in the lower-dimensional problems.

More broadly, the lower-dimensional sub-problems tend to produce Pareto approximate sets that are near the extreme boundaries of the larger-dimensional problem. Sub-Figure 7a includes four sub-problems for which the Pareto approximate set consists of a single solution (J^{cash}-J^{hedge}, J^{cash}-J^{fund}, J^{hedge}-J^{fund}, J^{cash}-J^{hedge}-J^{fund}). Each of these sub-problems excludes debt, leading to a single optimal policy that performs essentially no risk management. This is consistent with prior work finding that conflicts in higher-dimensional problems can remain hidden in lower-dimensional sub-problems (Kollat & Reed, 2007; Matrosov et al., 2015; Woodruff et al., 2013). Sub-Figure 7a also shows results for the J^{cash}-J^{debt}, J^{debt}-J^{hedge}, and J^{debt}-J^{fund} sub-problems. Each subset of solutions is concentrated along an outer border of the larger Pareto front, where performance of the two explicitly-considered objectives is optimized at the expense of the other two objectives. The same pattern is evident in the 3-objective sub-problems of Sub-Figures 7b (J^{cash}-J^{debt}-J^{hedge}), 7c (J^{cash}-J^{debt}-J^{fund}), and 7d (J^{debt}-J^{hedge}-J^{fund}). These solution sets are larger, but still occupy extremal regions of the overall Pareto front. Thus, by choosing to optimize a 2- or 3-objective sub-problem, decision-makers may unwittingly produce an incomplete and biased Pareto approximate set.

The larger-dimensional problem leads to a fuller set of alternatives that better represents the tradeoffs associated with decision-maker preferences for different financial risk management tools. However, it is a non-trivial task to select a single operating policy from among the large Pareto approximate set. Interactive visualization approaches can help with this task. One example is to allow decision-makers to apply *a posteriori* performance criteria and "brush away" solutions that fail to meet these constraints (Kasprzyk, Nataraj, Reed, & Lempert, 2013). The strictness of the constraints can be iteratively increased until decision-makers are relatively agnostic about the tradeoffs across the feasible solution set. For example, consider a utility whose financial team (perhaps in consultation with its regulatory commission) develops the following criteria: if $\bar{R} = \$10.99$M is the mean annual net hydropower revenue in the absence of any risk management, then (1) the risk management policy should not reduce expected annualized cash flows by more than 2.5% ($J^{cash} \geq 0.975\bar{R}$); (2) the utility should rarely be forced to borrow more than 150% of mean net revenue to cover cash flow deficits ($J^{debt} \leq 1.5\bar{R}$); and (3) the utility should not maintain reserves larger 150% of mean net revenue ($J^{fund} \leq 1.5\bar{R}$). These constraints drastically reduce the set of feasible solutions (Figure 8). At this point, a quantitative method such as TOPSIS (Behzadian et al., 2012; Roszkowska, 2011) can be used to select one of the remaining policies for the utility to use (e.g., the policy outlined in Figure 8 and listed in Row 3 of Table 2).

While these constraints could, in theory, be applied *a priori* and used to reduce the number of objectives in the optimization, it is very difficult in practice for decision-

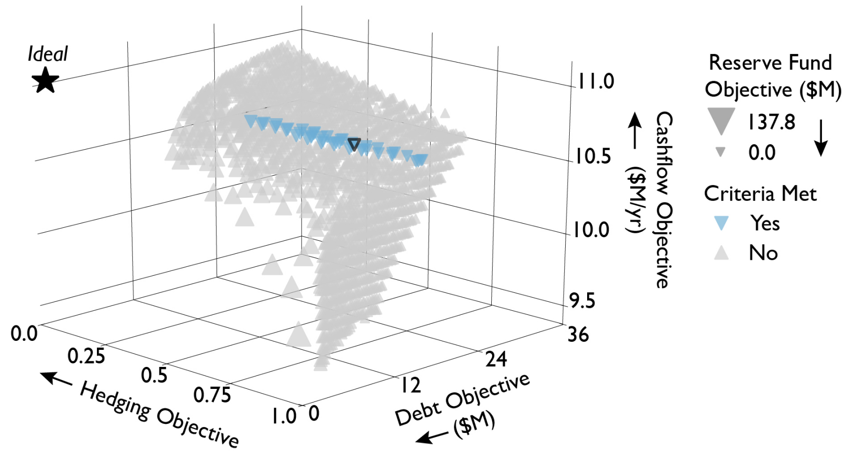

Figure 8. Set of feasible solutions after filtering for stakeholder-determined *a posteriori* constraints. The best compromise policy from the feasible set is outlined in black and described in Row 3 of Table 2

makers to effectively set the constraint values without first understanding the topology of the tradeoff surface (Kasprzyk et al., 2016; Spronk et al., 2005). This highlights the value of the EMODPS approach, which is scalable to extremely large problems on modern high-performance computing infrastructure (Giuliani et al., 2018; Zatarain Salazar et al., 2016), suggesting that the formulation used here could be expanded to include additional objectives such as customer rates, social equity, and environmental quality. Additionally, future work should consider the effects of alternative problem framings; for example, a decision-maker may prefer a risk metric based on cash flow semi-variance (Turvey & Nayak, 2003), or a hedging objective that seeks to maximize year-to-year stability for planning purposes (Quinn, Reed, & Keller, 2017). In practice, researchers and stakeholders can iteratively refine the multi-objective problem in a way that matches their intuitions and goals (Smith, Kasprzyk, & Dilling, 2017; Wu et al., 2016) while balancing the accuracy of the Monte Carlo estimator and the tractability of the search (Kasprzyk et al., 2012; Quinn, Reed, Giuliani, & Castelletti, 2017; Zatarain Salazar et al., 2017).

5.3 Value of state information for control

As demonstrated above, the EMODPS method can be used to develop control policies that perform well across a range of stakeholder preferences. However, decision-makers may be unwilling to adopt a complex, non-linear control policy if its operating rules remain opaque; it may be necessary to "open the black box" for users if they are to apply such tools in practice (Castelvecchi, 2016; Quinn et al., 2019). Each policy represents a map from a vector of inputs (e.g., reserve fund balance) to its outputs (e.g., the hedging contract slope). ITSA (Section 3.4) can help decision-makers to better understand how different policies respond to changing model state information. Figure 9 shows the hedging policy sensitivity indices for each solution in the Pareto approximate set, representing the degree to which each policy adjusts its annual hedging decision based on each of the three inputs: the reserve fund balance (η_F^H, Sub-Figure 9a), the debt (η_D^H, 9b), and the power price index (η_P^H, 9c). Each index is a measure of the importance of a particular input variable for controlling a state-aware policy; $\eta = 1$ implies that the policy is entirely controlled by the input, while $\eta = 0$ means that the input has no impact on the policy. Interestingly, Figure 9 shows that each input has a different region of "specialization" in objective space. The reserve fund balance is the most important input for policies along the top of the ridge where $J^{hedge} = 1$. These are policies that achieve a relatively low levels of debt and high levels of cash flow, in return for frequent hedging and a relatively large reserve fund. The debt information, on the other hand, is critical for policies occupying the swath of objective space with J^{hedge} between 0 and 1. The power price index is less informative overall, but does provide value for policies along the bottom edge of the Pareto front with minimal reserve funds and debt.

In order to better understand how these policies utilize information, it is helpful to visualize the policies themselves. One high-sensitivity policy is chosen for each input (as outlined in Figure 9, and listed in Rows 4-6 of Table 2). Each policy is used to simulate 20 random 20-year trajectories. The 400 resulting decisions are visualized in state-action space using parallel-coordinate plots (Figure 10). The first three vertical axes represent the three hedging policy inputs (reserve fund balance, debt, power price index). The policy output (hedging contract slope) is represented by the fourth vertical axis as well as the colorbar to aid interpretation. Each colored line connecting the four axes represents one of the 400 simulated decisions. These visualizations, in combination with the sensitivity indices, can be useful in understanding how each policy operates. For example, the policy in Sub-Figure 10a appears to hedge selectively, when the reserve fund balance has fallen below a certain threshold. Above the threshold, no hedging contract is purchased, and below the threshold, the hedging slope increases as the fund balance falls. The policy in Sub-Figure 10b has a similar strategy, but structured around debt; hedg-

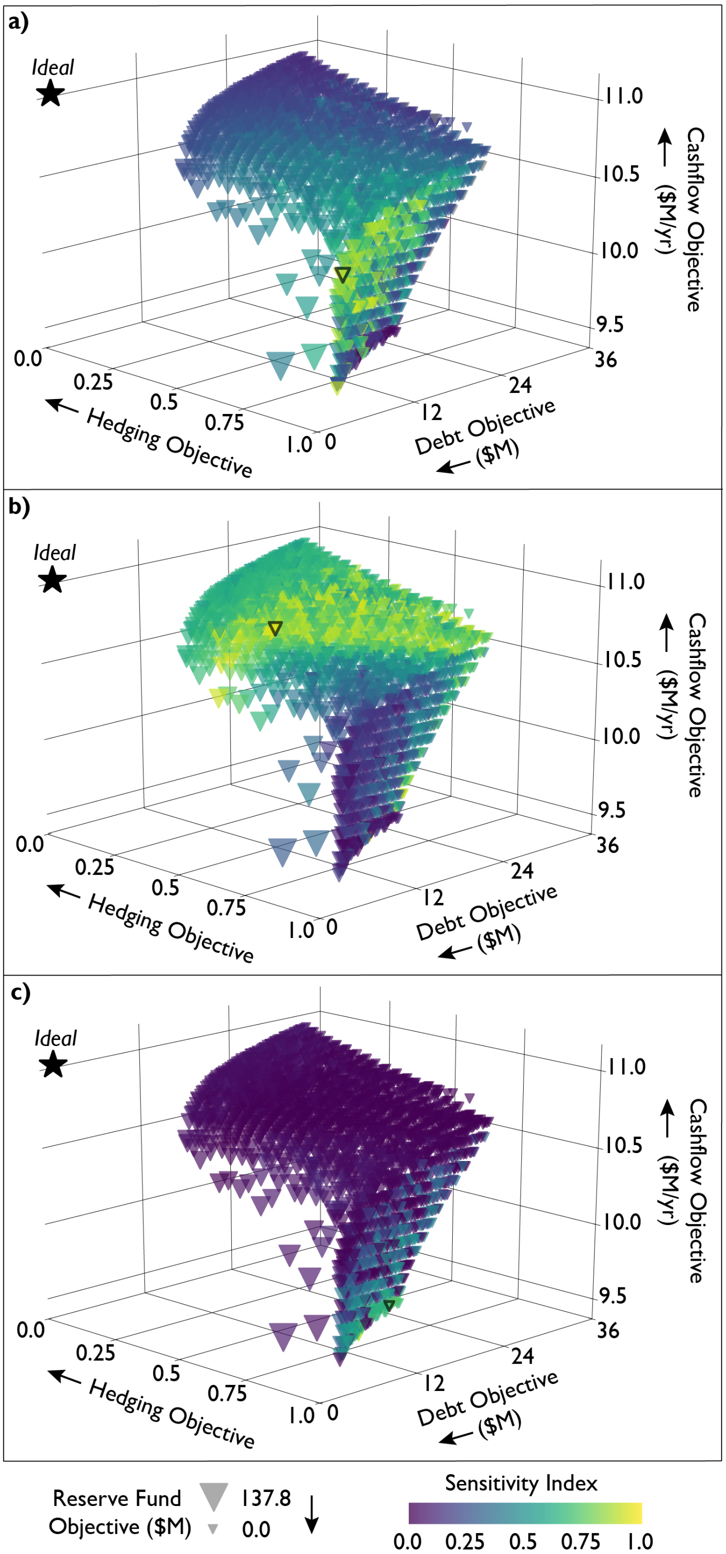

Figure 9. Information theoretic sensitivity indices, relative to hedging contract slope decision, for the (a) reserve fund balance; (b) debt; and (c) power price index. One high-sensitivity solution for each input is outlined in black and described in Rows 4-6 of Table 2

ing is zero below some threshold, and increases with debt above the threshold. Lastly, the bottom policy always utilizes hedging contracts, the magnitude of which tend to be inversely proportional to the power price index. Each of these patterns is consistent with the sensitivity indices in Figure 9 and Table 2.

These plots can be used to build intuition about how the different risk management policies achieve their competitive advantages. For example, compare the fund-sensitive policy (a) to the debt-sensitive policy (b). The former maintains a relatively large reserve fund for its risk management needs, and uses hedging contracts as a substitute to maintain its risk protection when the reserve fund is inadequate. This is qualitatively similar behavior to the example policy simulated in Section 5.1 (Figure 5). The debt-sensitive policy, on the other hand, keeps a much smaller reserve fund, which results in more frequent cash flow shortfalls and debt during dry years. In order to reduce the likelihood of extreme debt spirals during longer droughts, this policy begins to use hedging contracts when it has significant debt, and ceases hedging once it has paid off this debt. The result is that the debt-sensitive policy is significantly more risky than the fund-sensitive policy, but in return, it is less costly and requires less frequent hedging and a smaller reserve fund. The power-sensitive policy (c) takes a more consistent approach, purchasing hedging contracts each year. This makes it the most expensive policy of the three due to the cost of these contracts. However, the risk coverage from hedging allows it to maintain a very small reserve fund and still avoid substantial debt. This policy also adjusts its hedging contract in response to projected wholesale power prices. If the power price index is high, then the utility expects that its net revenue per unit of hydropower will be higher than average, and vice versa when the index is low. By purchasing hedging contracts in inverse proportion to this index, the utility can dampen the overall variability of its combined cash flow (hydropower net revenue plus the net payout from the hedging contract), and thus reduce its financial risk.

ITSA and policy visualization plots for the withdrawal/deposit decision can be found in SI Figures S6-S7. The withdrawals and deposits are found to be much less sensitive to model state information than hedging, suggesting that the gains from dynamic financial risk management in this study largely accrue from dynamic hedging rather than dynamic reserve fund management. This is consistent with past studies which have found relatively simple optimal control rules for cash inventory problems; however, such studies often employ strict assumptions on the distribution and predictability of incoming

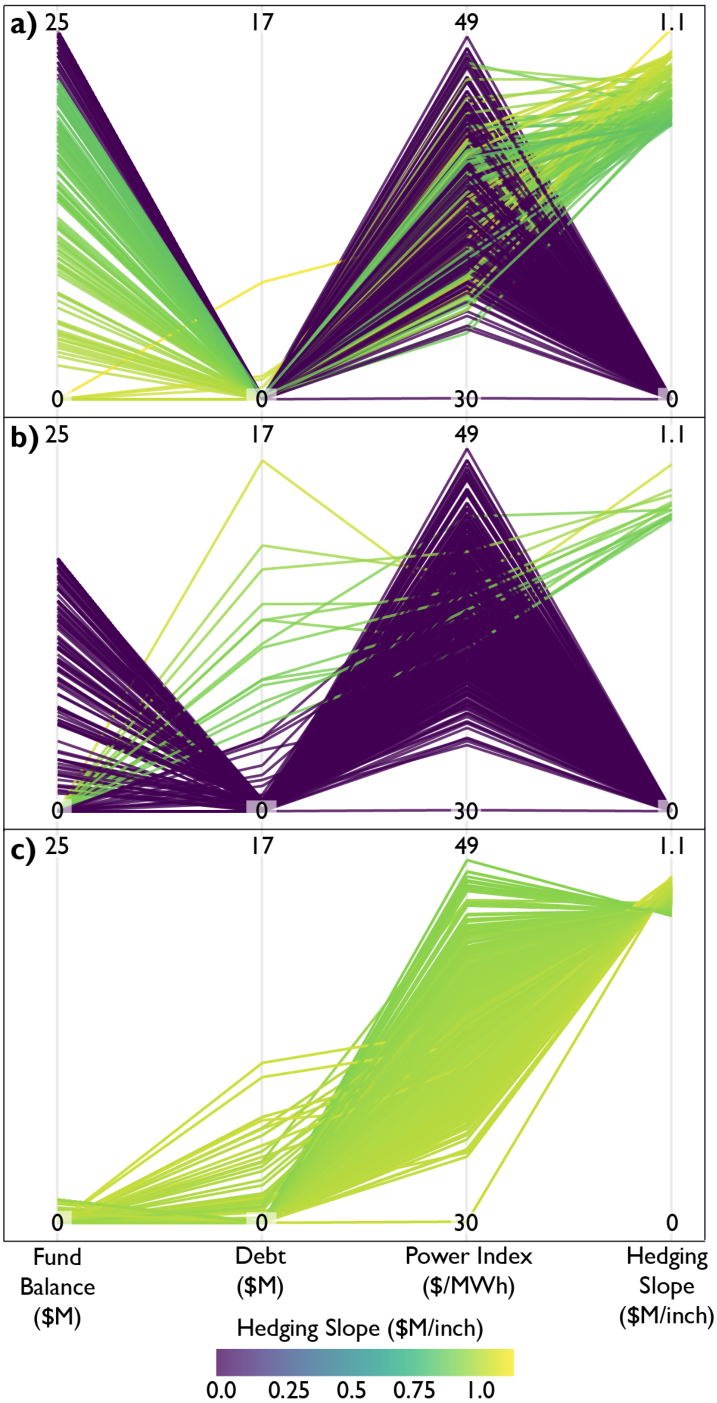

Figure 10. Hedging control policy visualization for three chosen policies in Figure 9 and Rows 4-6 of Table 2. Policies (a), (b), and (c) are highly sensitive to the reserve fund, debt, and power price index information, respectively. The first three vertical axes represent the three inputs, while the fourth axis and the colorbar represent the hedging action. Each line connecting the four axes represents one state-action combination experienced within a simulation.

cash flows, and their generalizability to real-world situations is uncertain (da Costa Moraes et al., 2015). A major advantage of the EMODPS approach is the flexibility of the non-linear approximating network used to parameterize the policies. The RBF network is found to identity complex policies for the hedging decision while maintaining relatively simple rules for the withdrawal/deposit decision (i.e., without over-fitting). This flexibility is important when the decision analyst does not know the optimal rule form for each action *a priori.* In problems with a larger number of candidate actions, an iterative scheme for selecting the decisions most amenable to dynamic control would be beneficial.

One final takeaway from Figures 9 and 10 is that the most important model states to include in a state-aware control policy can vary widely across the Pareto approximate set. This implies that the most important input(s) cannot be known *a priori* without accounting for decision-maker preferences. This is consistent with both analytical (Graham & Georgakakos, 2010; Tejada-Guibert, Johnson, & Stedinger, 1995) and empirical (Hejazi et al., 2008) studies in the reservoir control literature, which have found that the objective(s) of the operator can affect which hydrologic factors are deemed most informative. However, computational constraints often require that the total set of potentially informative data be culled to a small subset of the most important variables. The results of this study confirm the importance of accounting for the multi-dimensional nature of information value during this process (Denaro et al., 2017; Giuliani et al., 2015).

5.4 Limitations and future directions

A limitation of this study is that the stochastic engine adopted from Hamilton et al. (2020) assumes that wholesale power prices are independent from hydrology. In reality, fluctuations in hydropower availability can impact wholesale prices across the western United States on multiple timescales (Su, Kern, Reed, & Characklis, 2020; Voisin et al., 2018). This inverse correlation between streamflow and price could alter the utility's financial risk either for the better (e.g., higher prices received for hydropower sold during drought) or for the worse (e.g., higher prices paid for replacement power). Future work could integrate these factors into the adaptive hydro-financial risk model using an economic power dispatch model (e.g., Su, Kern, Denaro, et al. (2020)) or a surrogate statistical model (e.g., Madani, Guégan, and Uvo (2014)), but this is beyond the scope of the current investigation.

Another limitation of this study is the implicit assumption of stationarity embedded in the stochastic engine adopted from Hamilton et al. (2020). Despite this fact, Figure 5 suggests that the EMODPS-derived policies trained on a stationary Monte Carlo ensemble can perform relatively well across a wide range of potential outcomes, many of which are extreme compared to historical data. Additionally, the present study concerns purely financial decisions on relatively short time scales, for which interannual climate variability is expected to overwhelm longer-term non-stationarity (Lehner et al., 2020). The reader is referred to Hamilton et al. (2020) for further discussion of these issues. Nonetheless, future studies should consider a broader analysis of the impacts of changing climate, markets, etc., on the robustness of adaptive financial risk management strategies for hydropower production. This would be especially important if combined with dynamic infrastructure investments (Haasnoot, Kwakkel, Walker, & ter Maat, 2013; Kwakkel, Haasnoot, & Walker, 2015; Zeff, Herman, Reed, & Characklis, 2016), since climate uncertainties become increasingly important for long-term, irreversible decisions (Doss-Gollin, Farnham, Steinschneider, & Lall, 2019; Stakhiv, 2011). Statistical learning approaches can be used to update decision-making based on evolving beliefs about the non-stationary hydro-financial system (Cohen, Zeff, & Herman, 2020; Fletcher, Lickley, & Strzepek, 2019; Fletcher et al., 2017; Herman, Quinn, Steinschneider, Giuliani, & Fletcher, 2020). Additionally, scenario discovery approaches can be used to search for financial risk management strategies that perform satisfactorily across a wide range of (perhaps deeply) uncertain factors (Bryant & Lempert, 2010; Herman, Reed, Zeff, & Characklis, 2015; Kasprzyk et al., 2013; Lempert, 2002).

6 Conclusions

A substantial body of literature has emerged around optimal control of water reservoir systems in the face of hydrologic uncertainty (Macian-Sorribes & Pulido-Velazquez, 2019). Evolutionary multi-objective direct policy search has emerged as an especially powerful tool for overcoming the simultaneous curses of dimensionality, modeling, and multiple objectives that are characteristic of problems in the field (Giuliani et al., 2016, 2018). This paper demonstrates that the same properties of EMODPS that make it ideal for optimal reservoir control problems also make it well suited for the complex, multi-objective financial risk management problems faced by water-reliant organizations as a result of hydrologic variability. The methodology is applied in the context of the hydrologic financial risk faced by the Power Enterprise of the San Francisco Public Utilities Commission, an electricity producer relying primarily on hydropower. EMODPS is used to develop control policies that dynamically balance the use of snowpack-based hedging contracts, cash reserves, and debt, based on changing conditions within the model. Performance is quantified based on four conflicting performance metrics: expected annualized cash flow, 95th percentile maximum debt, expected hedging frequency, and expected maximum reserve fund balance. The first two metrics represent the classic return vs. risk tradeoff in finance, while the second two metrics represent a decision-maker's preferences for using one risk management instrument over another based on an organization's individual circumstances. By utilizing real-time model state information when making decisions, the dynamic policies produced by EMODPS are found to significantly outperform policies produced under a more static control formulation akin to those commonly used for financial risk management in the water resources literature. *A posteriori* visual analytics and information theoretic sensitivity analysis can be used to help decision-makers better understand how the complex, non-linear operating policies adapt to real-time information when making decisions.

The methodology developed in this paper should help decision-makers to better understand the dynamic relationships between hydrology, decision-making, and financial outcomes, and thus facilitate more knowledgeable and effective management of hydrologic financial risks. Additionally, we note that while the interrelatedness of hydrology and financial risk is conceptually useful for the present study (i.e., water resources researchers and practitioners will easily grasp the similarities between reservoir control and financial risk management), it does not represent a necessary condition for the usefulness of the dynamic financial risk management framework presented herein. In fact, a broad class of financial risk management problems share a similar mathematical structure to reservoir control (i.e., multi-objective Markov Decision Processes). Although the decision-making context and implementation details will vary, the overall framework presented here should thus be applicable to a wide variety of organizations, from water utilities exposed to hydrologic risk, to renewable energy developers exposed to wind risk, to commodities firms exposed to interest rate risk.

Acknowledgments

Funding for this work was provided by the National Science Foundation (NSF), Innovations at the Nexus of Food-Energy-Water Systems, Track 2 (Award 1639268). The authors would like to thank Rohini Gupta for helpful discussion and code review, as well as Alexis Dufour and Darryl Dunn from the San Francisco Public Utilities Commission (SFPUC) for helpful discussion and data provision. The views expressed in this work represent those of the authors and do not necessarily reflect the views or policies of the NSF or SFPUC. All code and data for this project, including figure generation, are available in a live repository (`https://github.com/ahamilton144/hamilton-2021-EMODPS-financial-risk`) and a permanent archive (`https://doi.org/10.5281/zenodo.5079786`).

References

Aguilar-Rivera, R., Valenzuela-Rendón, M., & Rodríguez-Ortiz, J. J. (2015, 6). Genetic algorithms and Darwinian approaches in financial applications: A survey. *Expert Systems with Applications*, *42*(21), 7684–7697. doi: 10.1016/j.eswa.2015.06.001

Auder, B., & Iooss, B. (2009). Global sensitivity analysis based on entropy. *Safety, Reliability and Risk Analysis: Theory, Methods and Applications - Proceedings of the Joint ESREL and SRA-Europe Conference*, *3*, 2107–2115.

Bank, M., & Wiesner, R. (2010). The Use of Weather Derivatives by Small-and Medium- Sized Enterprises: Reasons and Obstacles. *Journal of Small Business and Entrepreneurship*, *23*(4), 581–600. doi: 10.1080/08276331.2010.10593503

Basdekas, L. (2014). Is multiobjective optimization ready for water resources practitioners? Utility's drought policy investigation. *Journal of Water Resources Planning and Management*, *140*(3), 275–276. doi: 10.1061/(ASCE)WR.1943-5452.0000415

Basdekas, L., & Hayslett, R. (2021). *Improving Tradeoff Understanding in Water Resource Planning Using Multi-Objective Search* (Tech. Rep.).

Baumol, W. J. (1952). The Transactions Demand for Cash : An Inventory Theoretic Approach. *The Quarterly Journal of Economics*, *66*(4), 545–556.

Behzadian, M., Khanmohammadi Otaghsara, S., Yazdani, M., & Ignatius, J. (2012, 12). A state-of-the-art survey of TOPSIS applications. *Expert Systems with Applications*, *39*, 13051–13069. doi: 10.1016/j.eswa.2012.05.056

Bellman, R. (1957). *Dynamic Programming.* Princeton, NJ: Princeton University Press.

Bertsekas, D. P. (2019). *Reinforcement learning and optimal control.* Nashua, NH: Athena Scientific.

Blomfield, A., & Plummer, J. (2014). The allocation and documentation of hydrological risk. *Hydropower & Dams*(5), 94–108. doi: 10.1093/rfs/15.4.1283

Bodnar, G. M., Giambona, E., Graham, J. R., & Harvey, C. R. (2019). A view inside corporate risk management. *Management Science*, *65*(11), 5001–5026. doi: 10.1287/mnsc.2018.3081

Bolton, P., Chen, H., & Wang, N. (2011). A Unified Theory of Tobin's q, Corporate Investment, Financing, and Risk Management. *Journal of Finance*, *66*(5), 1545–1578. doi: 10.1111/j.1540-6261.2011.01681.x

Borgonovo, E. (2007). A new uncertainty importance measure. *Reliability Engineering and System Safety*, *92*(6), 771–784. doi: 10.1016/j.ress.2006.04.015

Borgonovo, E., Castaings, W., & Tarantola, S. (2011). Moment Independent Importance Measures: New Results and Analytical Test Cases. *Risk Analysis*, *31*(3), 404–428. doi: 10.1111/j.1539-6924.2010.01519.x

Brown, C. M., & Carriquiry, M. (2007). Managing hydroclimatological risk to water supply with option contracts and reservoir index insurance. *Water Resources Research*, *43*, W11423. doi: 10.1029/2007WR006093

Brown, C. M., Lund, J. R., Cai, X., Reed, P. M., Zagona, E. A., Ostfeld, A., ... Brekke, L. (2015). The future of water resources systems analysis: Toward a scientific framework for sustainable water management. *Water Resources Research*, *51*(8), 6110–6124. doi: 10.1002/2015WR017114

Bryant, B. P., & Lempert, R. J. (2010). Thinking inside the box: A participatory, computer-assisted approach to scenario discovery. *Technological Forecasting and Social Change*, *77*(1), 34–49. doi: 10.1016/j.techfore.2009.08.002

Cai, X., Wallington, K., Shafiee-Jood, M., & Marston, L. (2018). Understanding and managing the food-energy-water nexus - opportunities for water resources research. *Advances in Water Resources*, *111*(November), 259–273. doi: 10.1016/j.advwatres.2017.11.014

Castelletti, A., Pianosi, F., & Soncini-Sessa, R. (2008). Water reservoir control under economic, social and environmental constraints. *Automatica*, *44*(6), 1595–

1607. doi: 10.1016/j.automatica.2008.03.003

Castelletti, A., & Soncini-Sessa, R. (2006). A procedural approach to strengthening integration and participation in water resource planning. *Environmental Modelling and Software*, *21*(10), 1455–1470. doi: 10.1016/j.envsoft.2005.07.013

Castelvecchi, D. (2016). Can we open the black box of AI? *Nature*, *538*(7623), 20–23. doi: 10.1038/538020a

Ceres. (2017). *The Investor Water Toolkit* (Tech. Rep.). Boston, MA: Ceres. Retrieved from `https://www.ceres.org/sites/default/files/reports/Ceres_InvestWaterToolkit.pdf`

Chapman, T. A., & Breeding, J. M. (2014). *U.S. Public Finance Waterworks, Sanitary Sewer, and Drainage Utility Systems: Methodology And Assumptions* (Tech. Rep.). Standard and Poor's Ratings Services. Retrieved from `https://www.spratings.com/documents/20184/908554/US_PF_Event_RFCRndTblsJan2015_Article1/30d125eb-1066-4730-8ab1-f2cd6a6d6f9a`

Coello Coello, C. A., Lamont, G. B., & Van Veldhuizen, D. A. (2007). *Evolutionary Algorithms for Solving Multi-Objective Problems* (2nd ed.). New York, NY: Springer Science+Business Media, LLC. doi: 10.1046/j.1365-2672.2000.00969.x

Cohen, J. S., Zeff, H. B., & Herman, J. D. (2020). Adaptation of Multiobjective Reservoir Operations to Snowpack Decline in the Western United States. *Journal of Water Resources Planning and Management*, *146*(12), 04020091. doi: 10.1061/(asce)wr.1943-5452.0001300

da Costa Moraes, M. B., & Nagano, M. S. (2013). Cash Management Policies By Evolutionary Models: A Comparison Using The Miller-Orr Model. *Journal of Information Systems and Technology Management*, *10*(3), 561–576. doi: 10.4301/s1807-17752013000300006

da Costa Moraes, M. B., Nagano, M. S., & Sobreiro, V. A. (2015). Stochastic Cash Flow Management Models: A Literature Review Since the 1980s. In P. Guarnieri (Ed.), *Decision models in engineering and management* (pp. 11–28). Springer International Publishing Switzerland. doi: 10.1007/978-3-319-11949-6{_}2

de Almeida-Filho, A. T., de Lima Silva, D. F., & Ferreira, L. (2020). Financial modelling with multiple criteria decision making: A systematic literature review. *Journal of the Operational Research Society*, 1–19. doi: 10.1080/01605682.2020.1772021

Denaro, S., Anghileri, D., Giuliani, M., & Castelletti, A. (2017). Informing the operations of water reservoirs over multiple temporal scales by direct use of hydro-meteorological data. *Advances in Water Resources*, *103*, 51–63. doi: 10.1016/j.advwatres.2017.02.012

Denaro, S., Castelletti, A., Giuliani, M., & Characklis, G. (2020). Insurance Portfolio Diversification Through Bundling for Competing Agents Exposed to Uncorrelated Drought and Flood Risks. *Water Resources Research*, *56*(5), 1–20. doi: 10.1029/2019WR026443

Desreumaux, Q., Côté, P., & Leconte, R. (2018). Comparing model-based and model-free streamflow simulation approaches to improve hydropower reservoir operations. *Journal of Water Resources Planning and Management*, *144*(3), 1–10. doi: 10.1061/(ASCE)WR.1943-5452.0000860

di Pierro, F., Khu, S. T., & Savić, D. A. (2007). An investigation on preference order ranking scheme for multiobjective evolutionary optimization. *IEEE Transactions on Evolutionary Computation*, *11*(1), 17–45. doi: 10.1109/TEVC.2006.876362

Disatnik, D., Duchin, R. A. N., & Schmidt, B. (2014). Cash Flow Hedging and Liquidity Choices. *Review of Finance*, *18*, 715–748. doi: 10.1093/rof/rft006

D'Odorico, P., Davis, K. F., Rosa, L., Carr, J. A., Chiarelli, D., Dell'Angelo, J., … Rulli, M. C. (2018). The Global Food-Energy-Water Nexus. *Reviews of Geophysics*, *56*(3), 456–531. doi: 10.1029/2017RG000591

Doss-Gollin, J., Farnham, D. J., Steinschneider, S., & Lall, U. (2019). Robust Adaptation to Multiscale Climate Variability. *Earth's Future*, *7*(7), 734–747. doi: 10.1029/2019EF001154

Fabozzi, F. J., Focardi, S., & Jonas, C. (2007). Trends in quantitative equity management: Survey results. *Quantitative Finance*, *7*(2), 115–122. doi: 10.1080/14697680701195941

Fletcher, S., Lickley, M., & Strzepek, K. (2019). Learning about climate change uncertainty enables flexible water infrastructure planning. *Nature Communications*, *10*(1), 1–11. doi: 10.1038/s41467-019-09677-x

Fletcher, S., Miotti, M., Swaminathan, J., Klemun, M., Strzepek, K., & Siddiqi,

A. (2017). Water supply infrastructure planning decision-making framework to classify multiple uncertainties and evaluate flexible design. *Journal of Water Resources Planning and Management*, *143*(10), 04017061. doi: 10.1061/(ASCE)WR.1943-5452.0000823

Flood, M. D., Lemieux, V. L., Varga, M., & William Wong, B. L. (2016). The application of visual analytics to financial stability monitoring. *Journal of Financial Stability*, *27*, 180–197. doi: 10.1016/j.jfs.2016.01.006

Foster, B. T., Kern, J. D., & Characklis, G. W. (2015). Mitigating hydrologic financial risk in hydropower generation using index-based financial instruments. *Water Resources and Economics*, *10*, 45–67. doi: 10.1016/j.wre.2015.04.001

Froot, K., Scharfstein, D., & Stein, J. (1993). Risk Management: Coordinating Corporate Investment and Financing Policies. *The Journal of Finance*, *48*(5), 1629–1648. doi: 10.1111/j.1540-6261.1993.tb05123.x

Giuliani, M., & Castelletti, A. (2016). Is robustness really robust? How different definitions of robustness impact decision-making under climate change. *Climatic Change*, *135*(3-4), 409–424. doi: 10.1007/s10584-015-1586-9

Giuliani, M., Castelletti, A., Pianosi, F., Mason, E., & Reed, P. M. (2016). Curses, tradeoffs, and scalable management: Advancing evolutionary multiobjective direct policy search to improve water reservoir operations. *Journal of Water Resources Planning and Management*, *142*(2), 04015050. doi: 10.1061/(ASCE)WR.1943-5452.0000570

Giuliani, M., Herman, J. D., Castelletti, A., & Reed, P. (2014). Many-objective reservoir policy identification and refinement to reduce policy inertia and myopia in water management. *Water Resources Research*, *50*(4), 3355–3377. doi: 10.1002/2013WR014700

Giuliani, M., Mason, E., Castelletti, A., Pianosi, F., & Soncini-Sessa, R. (2014). Universal approximators for direct policy search in multi-purpose water reservoir management: A comparative analysis. In *Proceedings of the 19th world congress, international federation of automatic control* (Vol. 19, pp. 6234–6239). Cape Town, South Africa. doi: 10.3182/20140824-6-za-1003.01962

Giuliani, M., Pianosi, F., & Castelletti, A. (2015). Making the most of data: An information selection and assessment framework to improve water systems operations. *Water Resources Research*, *51*(11), 9073–9093. doi:

10.1002/2015WR017044

Giuliani, M., Quinn, J. D., Herman, J. D., Castelletti, A., & Reed, P. M. (2018). Scalable Multiobjective Control for Large-Scale Water Resources Systems under Uncertainty. *IEEE Transactions on Control Systems Technology*, *26*(4), 1492–1499. doi: 10.1109/TCST.2017.2705162

Graham, N. E., & Georgakakos, K. P. (2010). Toward understanding the value of climate information for multiobjective reservoir management under present and future climate and demand scenarios. *Journal of Applied Meteorology and Climatology*, *49*(4), 557–573. doi: 10.1175/2009JAMC2135.1

Gupta, R. S., Hamilton, A. L., Reed, P. M., & Characklis, G. W. (2020). Can modern multi-objective evolutionary algorithms discover high-dimensional financial risk portfolio tradeoffs for snow-dominated water-energy systems? *Advances in Water Resources*, *145*, 103718. doi: 10.1016/j.advwatres.2020.103718

Haasnoot, M., Kwakkel, J. H., Walker, W. E., & ter Maat, J. (2013). Dynamic adaptive policy pathways: A method for crafting robust decisions for a deeply uncertain world. *Global Environmental Change*. doi: 10.1016/j.gloenvcha.2012.12.006

Hadka, D., & Reed, P. (2012). Diagnostic assessment of search controls and failure modes in many-objective evolutionary optimization. *Evolutionary Computation*, *20*(3), 423–452. doi: 10.1162/EVCO{_}a{_}00053

Hadka, D., & Reed, P. (2013). Borg: An auto-adaptive many-objective evolutionary computing framework. *Evolutionary Computation*, *21*(2), 231–259. doi: 10.1162/EVCO{_}a{_}00075

Hamilton, A. L., Characklis, G. W., & Reed, P. M. (2020). Managing financial risk tradeoffs for hydropower generation using snowpack-based index contracts. *Water Resources Research*, *56*, e2020WR027212. doi: 10.1029/2020wr027212

Hejazi, M. I., Cai, X., & Ruddell, B. L. (2008). The role of hydrologic information in reservoir operation - Learning from historical releases. *Advances in Water Resources*, *31*(12), 1636–1650. doi: 10.1016/j.advwatres.2008.07.013

Herman, J. D., Quinn, J. D., Steinschneider, S., Giuliani, M., & Fletcher, S. (2020). Climate adaptation as a control problem: Review and perspectives on dynamic water resources planning under uncertainty. *Water Resources Research*, *56*, e24389. doi: 10.1029/2019wr025502

Herman, J. D., Reed, P. M., Zeff, H. B., & Characklis, G. W. (2015). How should robustness be defined for water systems planning under change? *Journal of Water Resources Planning and Management*, *141*(10), 04015012. doi: 10.1061/(ASCE)WR.1943-5452.0000509

Herman, J. D., Zeff, H. B., Reed, P. M., & Characklis, G. W. (2014). Beyond optimality: Multistakeholder robustness tradeoffs for regional water portfolio planning under deep uncertainty. *Water Resources Research*, *50*(10), 7692–7713. doi: 10.1002/2014WR015338

Hughes, J., & Leurig, S. (2013). *Assessing water system revenue risk: Considerations for market analysts* (Tech. Rep.). Boston, MA: Ceres and Environmental Finance Center at the University of North Carolina at Chapel Hill.

Hughes, J., Tiger, M., Eskaf, S., Berahzer, S. I., Royster, S., Boyle, C., & Batten, D. (2014). *Defining a Resilient Business Model for Water Utilities* (Tech. Rep.). Water Research Foundation. Retrieved from `https://efc.sog.unc.edu/sites/default/files/4366_Exec_Summary_0.pdf`

Hull, J. C. (2009). *Options, Futures, and Other Derivatives* (8th ed.). Boston, MA: Prentice Hall.

Huskova, I., Matrosov, E. S., Harou, J. J., Kasprzyk, J. R., & Lambert, C. (2016). Screening robust water infrastructure investments and their trade-offs under global change: A London example. *Global Environmental Change*, *41*, 216–227. doi: 10.1016/j.gloenvcha.2016.10.007

Iooss, B., & Lemaître, P. (2015). A review on global sensitivity analysis methods. *Operations Research/ Computer Science Interfaces Series*, *59*, 101–122. doi: 10.1007/978-1-4899-7547-8{_}5

Kasprzyk, J. R., Nataraj, S., Reed, P. M., & Lempert, R. J. (2013). Many objective robust decision making for complex environmental systems undergoing change. *Environmental Modelling and Software*, *42*, 55–71. doi: 10.1016/j.envsoft.2012.12.007

Kasprzyk, J. R., Reed, P. M., Characklis, G. W., & Kirsch, B. R. (2012). Many-objective de Novo water supply portfolio planning under deep uncertainty. *Environmental Modelling and Software*, *34*, 87–104. doi: 10.1016/j.envsoft.2011.04.003

Kasprzyk, J. R., Reed, P. M., & Hadka, D. M. (2016). Battling Arrow's Paradox to discover robust water management alternatives. *Journal of Water Resources Planning and Management*, *142*(2), 04015053. doi: 10.1061/(ASCE)WR.1943-5452.0000572

Kollat, J. B., & Reed, P. (2007). A framework for Visually Interactive Decision-making and Design using Evolutionary Multi-objective Optimization (VIDEO). *Environmental Modelling and Software*, *22*(12), 1691–1704. doi: 10.1016/j.envsoft.2007.02.001

Koutsoyiannis, D., & Economou, A. (2003). Evaluation of the parameterization-simulation-optimization approach for the control of reservoir systems. *Water Resources Research*, *39*(6). doi: 10.1029/2003WR002148

Kouwenberg, R., & Zenios, S. A. (2008). Stochastic Programming Models for Asset Liability Management. In *Handbook of asset and liability management* (Vol. 1, pp. 253–303). doi: 10.1016/B978-044453248-0.50012-5

Krause, T. A., & Tse, Y. (2016). Risk management and firm value: Recent theory and evidence. *International Journal of Accounting and Information Management*, *24*(1), 56–81. doi: 10.1108/IJAIM-05-2015-0027

Krzykacz-Hausmann, B. (2001). Epistemic sensitivity analysis based on the concept of entropy. In P. Prado & R. Bolado (Eds.), *Proceedings of samo* (pp. 31–35). Madrid: CIEMAT.

Kwakkel, J. H., Haasnoot, M., & Walker, W. E. (2015). Developing dynamic adaptive policy pathways: a computer-assisted approach for developing adaptive strategies for a deeply uncertain world. *Climatic Change*. doi: 10.1007/s10584-014-1210-4

Labadie, J. W. (2004). Optimal operation of multireservoir systems: State-of-the-art review. *Journal of Water Resources Planning and Management*, *130*(2), 93–111. doi: 10.1061/(ASCE)0733-9496(2004)130:2(93)

Larson, W. M., Freedman, P. L., Passinsky, V., Grubb, E., & Adriaens, P. (2012). Mitigating corporate water risk: Financial market tools and supply management strategies. *Water Alternatives*, *5*(3), 582–602.

Lehner, F., Deser, C., Maher, N., Marotzke, J., Fischer, E., Brunner, L., ... Hawkins, E. (2020). Partitioning climate projection uncertainty with multiple Large Ensembles and CMIP5/6. *Earth System Dynamics*, *11*, 491–508. doi: 10.5194/esd-2019-93

Lempert, R. J. (2002). A new decision sciences for complex systems. *Proceedings of the National Academy of Sciences of the United States of America*, *99*(SUPPL. 3), 7309–7313. doi: 10.1073/pnas.082081699

Leurig, S. (2010). *The Ripple Effect: Water risk in the municipal bond market* (Tech. Rep.). Boston, MA: Ceres. Retrieved from `https://www.ceres.org/resources/reports/ripple-effect-water-risk-municipal-bond-market`

Liu, H., Chen, W., & Sudjianto, A. (2006). Relative entropy based method for probabilistic sensitivity analysis in engineering design. *Journal of Mechanical Design*, *128*(2), 326–336.

Macian-Sorribes, H., & Pulido-Velazquez, M. (2019). Inferring efficient operating rules in multireservoir water resource systems: A review. *Wiley Interdisciplinary Reviews: Water*, *7*(1), e1400. doi: 10.1002/wat2.1400

Madani, K., Guégan, M., & Uvo, C. B. (2014). Climate change impacts on high-elevation hydroelectricity in California. *Journal of Hydrology*, *510*, 153–163. doi: 10.1016/j.jhydrol.2013.12.001

Maestro, T., Barnett, B. J., Coble, K. H., Garrido, A., & Bielza, M. (2016). Drought index insurance for the Central Valley Project in California. *Applied Economic Perspectives and Policy*, *38*(3), 521–545. doi: 10.1093/aepp/ppw013

Maier, H. R., Kapelan, Z., Kasprzyk, J., Kollat, J., Matott, L. S., Cunha, M. C., … Reed, P. M. (2014). Evolutionary algorithms and other metaheuristics in water resources: Current status, research challenges and future directions. *Environmental Modelling and Software*, *62*, 271–299. doi: 10.1016/j.envsoft.2014.09.013

Markowitz, H. (1952). Portfolio Selection. *The Journal of Finance*, *7*(1), 77–91.

Marqués, A. I., García, V., & Sánchez, J. S. (2020). Ranking-based MCDM models in financial management applications: analysis and emerging challenges. *Progress in Artificial Intelligence*, *9*(3), 171–193. doi: 10.1007/s13748-020-00207-1

Matrosov, E. S., Huskova, I., Kasprzyk, J. R., Harou, J. J., Lambert, C., & Reed, P. M. (2015). Many-objective optimization and visual analytics reveal key trade-offs for London's water supply. *Journal of Hydrology*, *531*, 1040–1053. doi: 10.1016/j.jhydrol.2015.11.003

Meyer, E. S., Characklis, G. W., Brown, C., & Moody, P. (2016). Hedging the financial risk from water scarcity for Great Lakes shipping. *Water Resources Research*, *52*(1), 227–245. doi: 10.1002/2015WR017855

Miller, M. M., & Orr, D. (1966). A Model of the Demand for Money by Firms. *The Quarterly Journal of Economics*, *80*(3), 413–435.

Moallemi, E. A., Kwakkel, J., de Haan, F. J., & Bryan, B. A. (2020, 11). Exploratory modeling for analyzing coupled human-natural systems under uncertainty. *Global Environmental Change*, *65*, 102186. doi: 10.1016/j.gloenvcha.2020.102186

Moody's Investors Service. (2011). *Rating Methodology: U.S. Public Power Electric Utilities with Generation Ownership Exposure* (Tech. Rep.).

Moody's Investors Service. (2019). *Bonneville Power Administration , OR: Credit Update Following Rating Affirmation and Change in Outlook to Negative* (Tech. Rep.).

Mortensen, E., & Block, P. (2018). ENSO Index-Based Insurance for Agricultural Protection in Southern Peru. *Geosciences*, *8*(2), 64. doi: 10.3390/geosciences8020064

Mulvey, J. M. (2001). Introduction to financial optimization: Mathematical Programming Special Issue. *Mathematical Programming*, *89*(2), 205–216. doi: 10.1007/pl00011395

Nicklow, J., Reed, P., Savic, D., Dessalegne, T., Harrell, L., Chan-Hilton, A., … Zechman, E. (2010). State of the Art for Genetic Algorithms and Beyond in Water Resources Planning and Management. *Journal of Water Resources Planning and Management*, *136*(4), 412–432. doi: 10.1061/ASCEWR.1943-5452.0000053

Pappenberger, F., Beven, K. J., Ratto, M., & Matgen, P. (2008). Multi-method global sensitivity analysis of flood inundation models. *Advances in Water Resources*, *31*(1), 1–14. doi: 10.1016/j.advwatres.2007.04.009

Pardalos, P. M., Sandström, M., & Zopounidis, C. (1994). On the use of optimization models for portfolio selection: A review and some computational results. *Computational Economics*, *7*(4), 227–244. doi: 10.1007/BF01299454

Pérez-González, F., & Yun, H. (2013). Risk management and firm value: Evidence from weather derivatives. *Journal of Finance*, *68*(5), 2143–2176. doi: 10.1111/jofi.12061

Pianosi, F., Beven, K., Freer, J., Hall, J. W., Rougier, J., Stephenson, D. B., & Wagener, T. (2016). Sensitivity analysis of environmental models: A systematic review with practical workflow. *Environmental Modelling and Software*, *79*, 214–232. doi: 10.1016/j.envsoft.2016.02.008

Ponsich, A., Jaimes, A. L., & Coello Coello, C. A. (2013). A survey on multiobjective evolutionary algorithms for the solution of the portfolio optimization problem and other finance and economics applications. *IEEE Transactions on Evolutionary Computation*, *17*(3), 321–344. doi: 10.1109/TEVC.2012.2196800

Powell, W. B. (2019). A unified framework for stochastic optimization. *European Journal of Operational Research*, *275*(3), 795–821. doi: 10.1016/j.ejor.2018.07.014

Quinn, J. D., Reed, P. M., Giuliani, M., & Castelletti, A. (2017). Rival framings: A framework for discovering how problem formulation uncertainties shape risk management trade-offs in water resources systems. *Water Resources Research*, *53*(8), 7208–7233. doi: 10.1002/2017WR020524

Quinn, J. D., Reed, P. M., Giuliani, M., & Castelletti, A. (2019). What Is Controlling Our Control Rules? Opening the Black Box of Multireservoir Operating Policies Using Time-Varying Sensitivity Analysis. *Water Resources Research*, *55*(7), 5962–5984. doi: 10.1029/2018WR024177

Quinn, J. D., Reed, P. M., Giuliani, M., Castelletti, A., Oyler, J. W., & Nicholas, R. E. (2018). Exploring How Changing Monsoonal Dynamics and Human Pressures Challenge Multireservoir Management for Flood Protection, Hydropower Production, and Agricultural Water Supply. *Water Resources Research*, *54*(7), 4638–4662. doi: 10.1029/2018WR022743

Quinn, J. D., Reed, P. M., & Keller, K. (2017). Direct policy search for robust multi-objective management of deeply uncertain socio-ecological tipping points. *Environmental Modelling and Software*, *92*, 125–141. doi: 10.1016/j.envsoft.2017.02.017

Rampini, A. A., Sufi, A., & Viswanathan, S. (2014). Dynamic risk management. *Journal of Financial Economics*, *111*(2), 271–296. doi: 10.1016/j.jfineco.2013.10.003

Reed, P. M., Hadka, D., Herman, J. D., Kasprzyk, J. R., & Kollat, J. B. (2013). Evolutionary multiobjective optimization in water resources: The past, present, and future. *Advances in Water Resources*, *51*, 438–456. doi: 10.1016/j.advwatres.2012.01.005

Rehan, R., Knight, M. A., Unger, A. J., & Haas, C. T. (2013). Development of a system dynamics model for financially sustainable management of municipal watermain networks. *Water Research*, *47*(20), 7184–7205. doi: 10.1016/j.watres.2013.09.061

Rehan, R., Unger, A., Knight, M. A., & Haas, C. (2015). Strategic water utility management and financial planning using a new system dynamics tool. *Journal - American Water Works Association*, *107*(1), E22-E36. doi: 10.5942/jawwa.2015.107.0006

Rosenstein, M. T., & Barto, A. G. (2001). Robot weightlifting by direct policy search. In *International joint conference on artificial intelligence* (pp. 839–844).

Roszkowska, E. (2011). Multi-criteria decision making models by applying the TOPSIS method to crisp and interval data. In *Multiple criteria decision making '10-11* (pp. 200–230). Publisher of The University of Economics in Katowice.

Rundo, F., Trenta, F., di Stallo, A. L., & Battiato, S. (2019, 12). Machine learning for quantitative finance applications: A survey. *Applied Sciences (Switzerland)*, *9*(24). doi: 10.3390/app9245574

Salas-Molina, F., Pla-Santamaria, D., & Rodriguez-Aguilar, J. A. (2018). A multi-objective approach to the cash management problem. *Annals of Operations Research*, *267*(1-2), 515–529. doi: 10.1007/s10479-016-2359-1

Saltelli, A., Tarantola, S., & Campolongo, F. (2000). Sensitivity Anaysis as an Ingredient of Modeling. *Statistical Science*, *15*(4), 377–395.

San Francisco Public Utilities Commission. (2016). *Comprehensive Annual Financial Report, Fiscal Years Ended June 30, 2016 and 2015* (Tech. Rep.).

Savikhin, A., Lam, H. C., Fisher, B., & Ebert, D. S. (2011). An experimental study of financial portfolio selection with visual analytics for decision support. *Proceedings of the Annual Hawaii International Conference on System Sciences*, 1–10. doi: 10.1109/HICSS.2011.54

Scanlon, B. R., Ruddell, B. L., Reed, P. M., Hook, R. I., Zheng, C., Tidwell, V. C., & Siebert, S. (2017). The food-energy-water nexus: Transforming science for society. *Water Resources Research*, *53*(5), 3550–3556. doi:

10.1002/2017WR020889

Shannon, C. (1948). A Mathematical Theory of Communication. *The Bell System Technical Journal*, *XXVII*(3), 379–423.

Singh, L. A., Whittecar, W. R., Diprinzio, M. D., Herman, J. D., Ferringer, M. P., & Reed, P. M. (2020). Low cost satellite constellations for nearly continuous global coverage. *Nature Communications*, *11*(200), 1–7. doi: 10.1038/s41467-019-13865-0

Smith, R., Kasprzyk, J., & Dilling, L. (2017). Participatory Framework for Assessment and Improvement of Tools (ParFAIT): Increasing the impact and relevance of water management decision support research. *Environmental Modelling and Software*, *95*, 432–446. doi: 10.1016/j.envsoft.2017.05.004

Smith, R., Kasprzyk, J., & Dilling, L. (2019). Testing the potential of Multiobjective Evolutionary Algorithms (MOEAs) with Colorado water managers. *Environmental Modelling and Software*, *117*, 149–163. doi: 10.1016/j.envsoft.2019.03.011

Sodhi, M. S. (2005). LP modeling for asset-liability management: A survey of choices and simplifications. *Operations Research*, *53*(2), 181–196. doi: 10.1287/opre.1040.0185

Spronk, J., Steuer, R. E., & Zopounidis, C. (2005). Multicriteria Decision Aid/Analysis in Finance. In *Multiple criteria decision analysis: State of the art surveys. international series in operations research & management science, vol. 78* (pp. 799–848). New York, NY: Springer.

Stakhiv, E. Z. (2011). Pragmatic approaches for water management under climate change uncertainty. *Journal of the American Water Resources Association*. doi: 10.1111/j.1752-1688.2011.00589.x

Su, Y., Kern, J. D., Denaro, S., Hill, J., Reed, P., Sun, Y., … Characklis, G. W. (2020). An open source model for quantifying risks in bulk electric power systems from spatially and temporally correlated hydrometeorological processes. *Environmental Modelling & Software*, *126*(January), 104667. Retrieved from `https://doi.org/10.1016/j.envsoft.2020.104667` doi: 10.1016/j.envsoft.2020.104667

Su, Y., Kern, J. D., Reed, P. M., & Characklis, G. W. (2020). Compound hydrometeorological extremes across multiple timescales drive volatility in California electricity market prices and emissions. *Applied Energy*, *276*(July), 115541. doi: 10.1016/j.apenergy.2020.115541

Sun, J., Fang, W., Wu, X., Lai, C. H., & Xu, W. (2011). Solving the multi-stage portfolio optimization problem with a novel particle swarm optimization. *Expert Systems with Applications*, *38*(6), 6727–6735. doi: 10.1016/j.eswa.2010.11.061

Tapia, M. G. C., & Coello Coello, C. A. (2007). Applications of multi-objective evolutionary algorithms in economics and finance: A survey. *2007 IEEE Congress on Evolutionary Computation*, 532–539. doi: 10.1109/CEC.2007.4424516

Tejada-Guibert, J. A., Johnson, S. A., & Stedinger, J. R. (1995). The Value of Hydrologic Information in Stochastic Dynamic Programming Models of a Multireservoir System. *Water Resources Research*, *31*(10), 2571–2579. doi: 10.1029/95WR02172

Turvey, C. G. (2001). Weather Derivatives for Specific Event Risks in Agriculture. *Review of Agricultural Economics*, *23*(2), 333–351. doi: 10.1111/1467-9353.00065

Turvey, C. G., & Nayak, G. (2003). The semivariance-minimizing hedge ratio. *Journal of Agricultural and Resource Economics*, *28*(1), 100–115. doi: 10.2307/40987175

Voisin, N., Kintner-Meyer, M., Wu, D., Skaggs, R., Fu, T., Zhou, T., … Kraucunas, I. (2018). Opportunities for joint water-energy management: Sensitivity of the 2010 western U.S. electricity grid operations to climate oscillations. *Bulletin of the American Meteorological Society*, *99*(2), 299–312. doi: 10.1175/BAMS-D-16-0253.1

Wild, T. B., Reed, P. M., Loucks, D. P., Mallen-Cooper, M., & Jensen, E. D. (2019). Balancing Hydropower Development and Ecological Impacts in the Mekong: Tradeoffs for Sambor Mega Dam. *Journal of Water Resources Planning and Management*, *145*(2), 05018019. doi: 10.1061/(asce)wr.1943-5452.0001036

Woodruff, M. J., Reed, P. M., & Simpson, T. W. (2013). Many objective visual analytics: Rethinking the design of complex engineered systems. *Structural and Multidisciplinary Optimization*, *48*, 201–219. doi: 10.1007/s00158-013-0891-z

Wu, W., Maier, H. R., Dandy, G. C., Leonard, R., Bellette, K., Cuddy, S., & Maheepala, S. (2016). Including stakeholder input in formulating and solving real-world optimisation problems: Generic framework and case study. *Environmental Modelling and Software*, *79*, 197–213. doi: 10.1016/j.envsoft.2016.02.012

Yeh, W. G. (1985). Reservoir Management and Operations Models: A State-of-the-Art Review. *Water Resources Research*, *21*(12), 1797–1818. doi: 10.1029/WR021i012p01797

Zatarain Salazar, J., Reed, P. M., Herman, J. D., Giuliani, M., & Castelletti, A. (2016). A diagnostic assessment of evolutionary algorithms for multi-objective surface water reservoir control. *Advances in Water Resources*, *92*, 172–185. doi: 10.1016/j.advwatres.2016.04.006

Zatarain Salazar, J., Reed, P. M., Quinn, J. D., Giuliani, M., & Castelletti, A. (2017). Balancing exploration, uncertainty and computational demands in many objective reservoir optimization. *Advances in Water Resources*, *109*, 196–210. doi: 10.1016/j.advwatres.2017.09.014

Zeff, H. B., & Characklis, G. W. (2013). Managing water utility financial risks through third-party index insurance contracts. *Water Resources Research*, *49*(8), 4939–4951. doi: 10.1002/wrcr.20364

Zeff, H. B., Herman, J. D., Reed, P. M., & Characklis, G. W. (2016). Cooperative drought adaptation: Integrating infrastructure development, conservation, and water transfers into adaptive policy pathways. *Water Resources Research*, *52*(9), 7327–7346. doi: 10.1002/2016WR018771

Zeff, H. B., Kasprzyk, J. R., Herman, J. D., Reed, P. M., & Characklis, G. W. (2014). Navigating financial and supply reliability tradeoffs in regional drought management portfolios. *Water Resources Research*, *50*(6), 4906–4923. doi: 10.1002/2013WR015126

Zopounidis, C., Doumpos, M., & Niklis, D. (2018). Financial decision support: an overview of developments and recent trends. *EURO Journal on Decision Processes*, *6*(1-2), 63–76. doi: 10.1007/s40070-018-0078-3

Zopounidis, C., Galariotis, E., Doumpos, M., Sarri, S., & Andriosopoulos, K. (2015). Multiple criteria decision aiding for finance: An updated bibliographic survey. *European Journal of Operational Research*, *247*(2), 339–348. doi: 10.1016/j.ejor.2015.05.032

Supporting Information for "From Stream Flows to Cash Flows: Leveraging Evolutionary Multi-Objective Direct Policy Search to Manage Hydrologic Financial Risk"

Andrew L. Hamilton[1,2], Gregory W. Characklis[1,2], and Patrick M. Reed[3]

[1]Department of Environmental Sciences and Engineering, University of North Carolina at Chapel Hill, Chapel Hill, North Carolina, USA

[2]Center on Financial Risk in Environmental Systems, University of North Carolina at Chapel Hill, Chapel Hill, North Carolina, USA

[3]Department of Civil and Environmental Engineering, Cornell University, Ithaca, New York, USA

Contents of this file

1. Text S1
2. Tables S1
3. Figures S1-S7

Corresponding author: Andrew L. Hamilton, `andrew.hamilton@unc.edu`

Introduction

This Supporting Information (SI) provides additional methodological details related to the power price index (Section S1), in support of Section 2.2 of the main text. Additionally, this SI provides Table S1 (supporting Section 4.2 of the main text), Figure S1 (supporting Section 2.1 of the main text), Figure S3 (supporting Section 2.2 of the main text and Section S1 of SI), Figure S3 (supporting Section 2.2 of the main text), Figure S4 (supporting Section 4.2 of the main text), Figure S5 (supporting Section 5.2 of the main text), and Figures S6-S7 (supporting Section 5.3 of the main text).

S1: Power price index

The power price index (ε^P, in \$/MWh) is the third stochastic driver described in Section 2.2 of the main text. Like the other two drivers, ε^P is derived from the one million years of monthly synthetic hydro-financial records from Hamilton, Characklis, and Reed (2020); specifically, it is based on the monthly time series of wholesale power price and hydropower generation.

Let $\bar{G}_m$ be the average excess hydropower sold into the wholesale market in month m. This quantity is highest in the spring and early summer, when the alpine snow melts. It is lowest, and negative, during the autumn dry season, when hydropower is often insufficient to meet retail electricity demand. The generation-weighted average power price for water year t is defined as

$$P_t^{wt} = \frac{1}{12} \frac{\sum_{m=1}^{12} \bar{G}_m P_{m,t}}{\sum_{m=1}^{12} \bar{G}_m} \tag{1}$$

where $P_{m,t}$ is the power price in the mth month of water year t (\$/MWh). P_t^{wt} will be highest for years in which dry-season power prices are lower than average and wet-season power prices are higher than average, both of which are generally beneficial from a net revenue perspective.

The generation-weighted average power price over the coming year can be predicted via linear regression in log-space, using information about power prices from the prior year:

$$\ln P_t^{wt} = \hat{\beta}_0 + \hat{\beta}_1 \ln P_{t-1}^{wt} + \hat{\beta}_2 \ln P_{12,t-1} + \epsilon \tag{2}$$

where $P_{12,t-1}$ is the power price in September, the final month of the prior water year, $\hat{\beta}_i$ are the estimated regression coefficients, and ϵ is the regression residual, assumed to follow a normal distribution with mean 0 and standard deviation σ.

Now the power price index is defined as the expected value of the generation-weighted average power price over the coming water year, conditional on the information from the prior year.

$$\begin{aligned}
\varepsilon_t^P &= E[P_t^{wt} \mid P_{t-1}^{wt},\ P_{12,t-1}] && (3)\\
&= E\left[\exp(\hat{\beta}_0 + \hat{\beta}_1 \ln P_{t-1}^{wt} + \hat{\beta}_2 \ln P_{12,t-1} + \epsilon)\right] && (4)\\
&= \exp(\hat{\beta}_0) \cdot (P_{t-1}^{wt})^{\hat{\beta}_1} \cdot (P_{12,t-1})^{\hat{\beta}_2} \cdot E[\exp(\epsilon)] && (5)\\
&= \exp(\hat{\beta}_0) \cdot (P_{t-1}^{wt})^{\hat{\beta}_1} \cdot (P_{12,t-1})^{\hat{\beta}_2} \cdot \exp(\sigma^2/2) && (6)
\end{aligned}$$

where σ is the standard deviation of the normally-distributed residuals from the log-space regression.

This power price index (in units of \$/MWh) thus predicts the generation-weighted average power price over the coming water year, t, using the information available from the prior water year, $t-1$. The performance of this index can be assessed by plotting the power price index against the realized generation-weighted average power price (Figure S2). This relationship is found to have a correlation coefficient of 0.35.

Tables

Table S1. Parameters for multi-objective optimization with the Borg Multi-Objective Evolutionary Algorithm.

Parameter	Value
Number of samples per function evaluation	50,000
Number of function evaluations per Borg MOEA run	150,000
Number of seeds for Borg MOEA	30
Number of radial basis functions (M)	2
Number of informational inputs to policy (L)	4
ϵ-dominance parameter for J^{cash}	\$0.075 M/year
ϵ-dominance parameters for J^{debt}	\$0.225 M
ϵ-dominance parameter for J^{hedge}	\$0.05001
ϵ-dominance parameters for J^{fund}	\$0.225 M

Figures

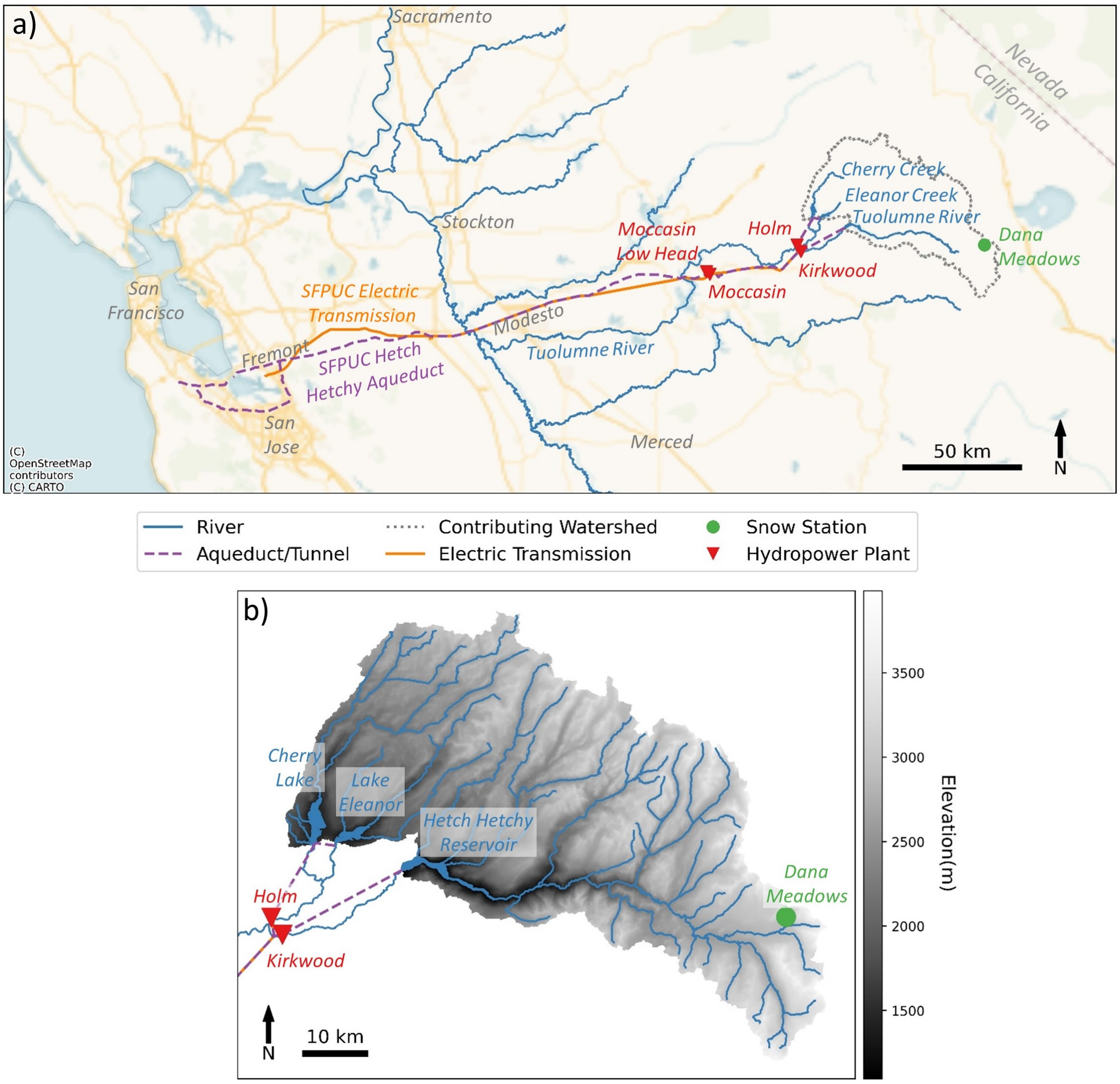

Figure S1. (a) Map of the study region. (b) Zoomed in map of the contributing watershed. Figure reproduced from Hamilton et al. (2020) Supporting Information.

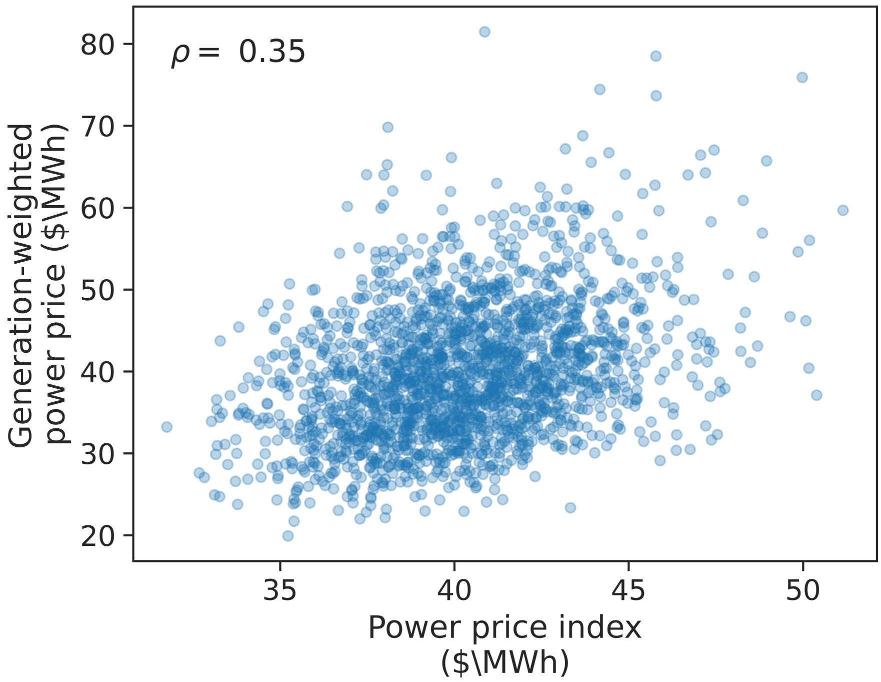

Figure S2. Relationship between power price index and generation-weighted average power price, along with correlation coefficient ρ. Only 2000 data points shown for clarity.

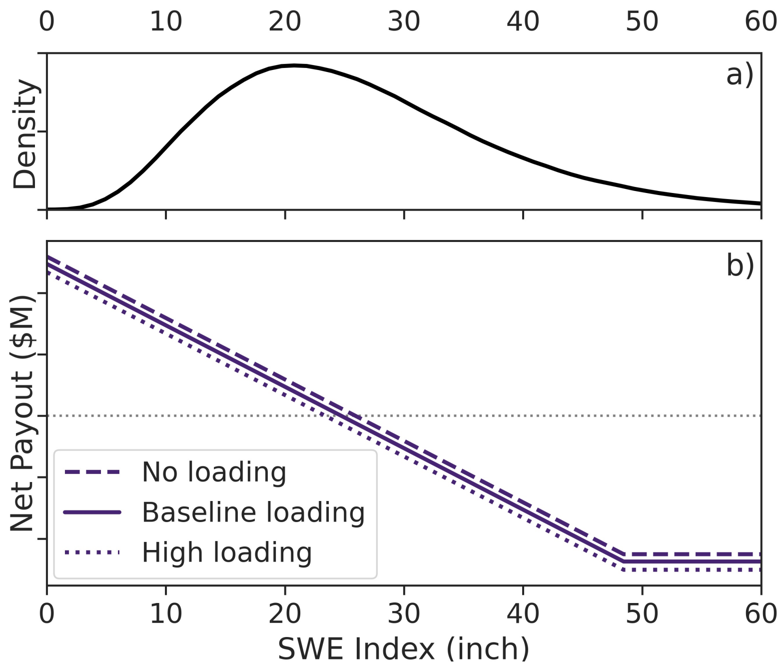

Figure S3. (a) Probability density for SWE index, a weighted average of February 1 and April 1 observations. (b) Net payout function for the capped contract for differences (CFD). The threshold separating positive and negative payouts is 24.71 inches. The slope of this contract is controlled by either the static or dynamic control policy. Present study uses the "baseline" loading. Figure adapted from Hamilton et al. (2020).

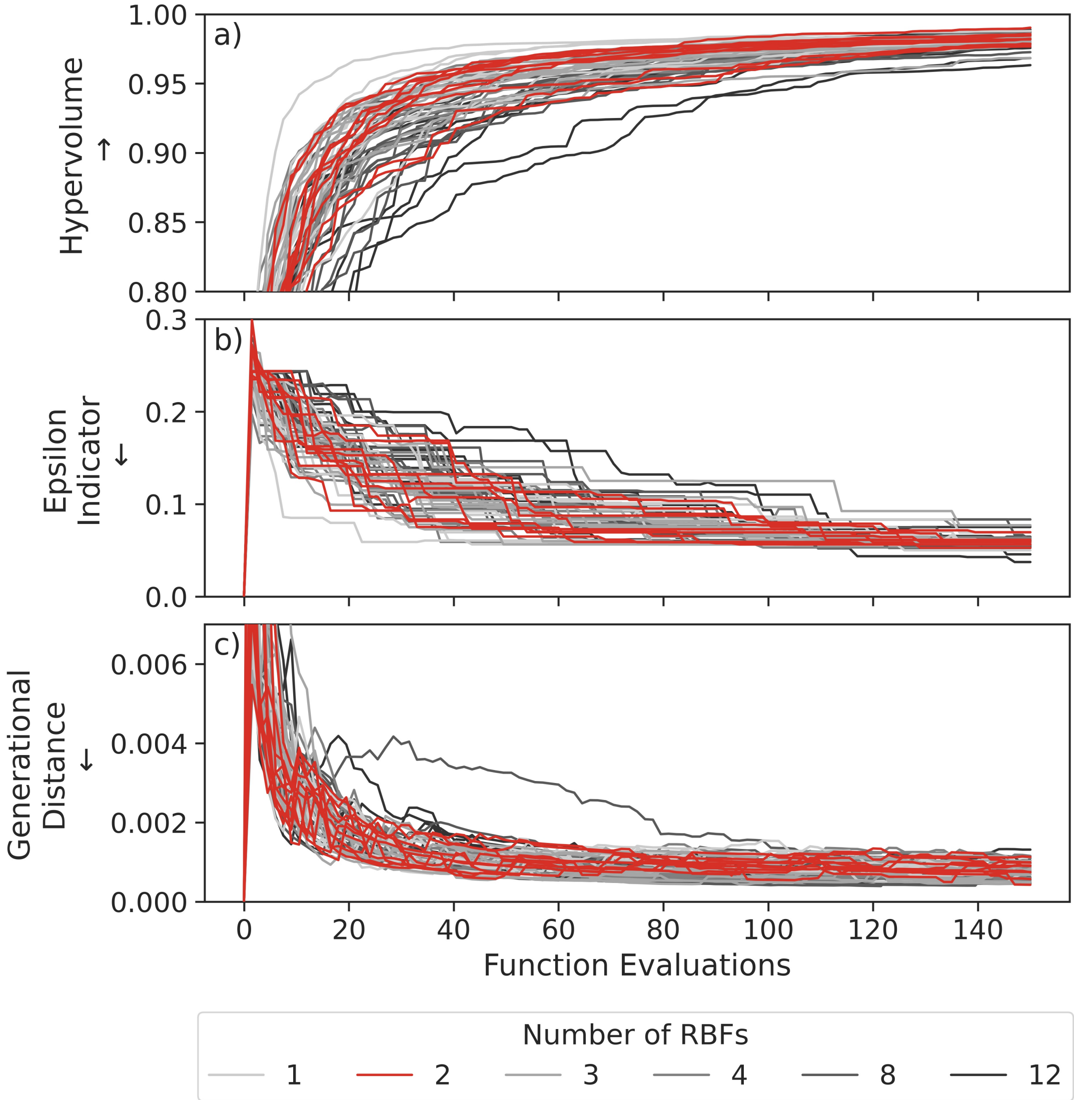

Figure S4. Convergence metrics for approximate Pareto sets from the Borg MOEA, using different numbers of radial basis functions (RBFs), for 10 random seeds each: (a) Hypervolume metric; (b) Generational distance metric; (c) Additive epsilon indicator metric.

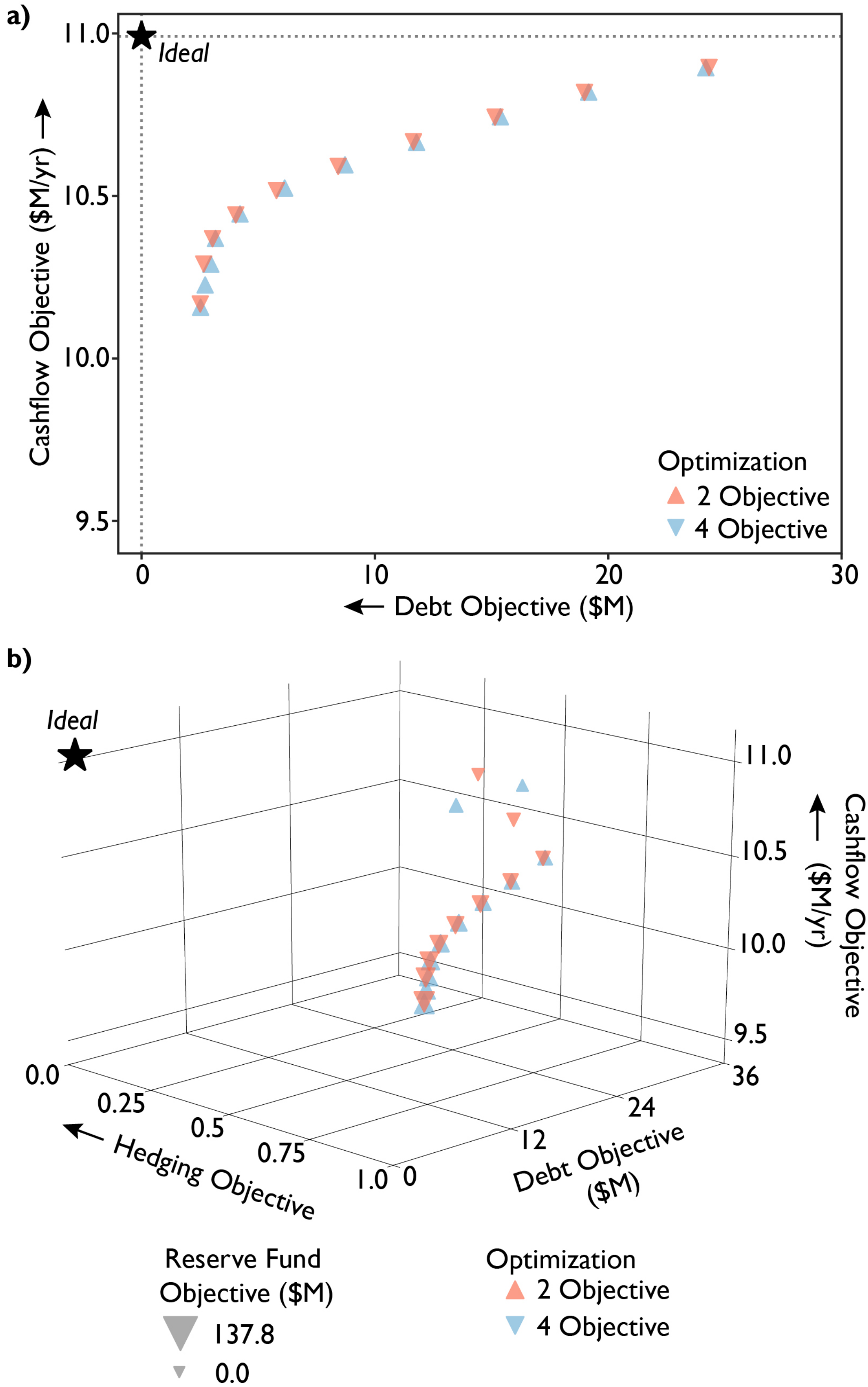

Figure S5. Results from 2-objective and 4-objective optimization problems, after filtering for non-dominated solutions with respect to the 2-objective problem (J^{cash} vs. J^{debt}). Results displayed for both 2-objective (a) and 4-objective (b) performance.

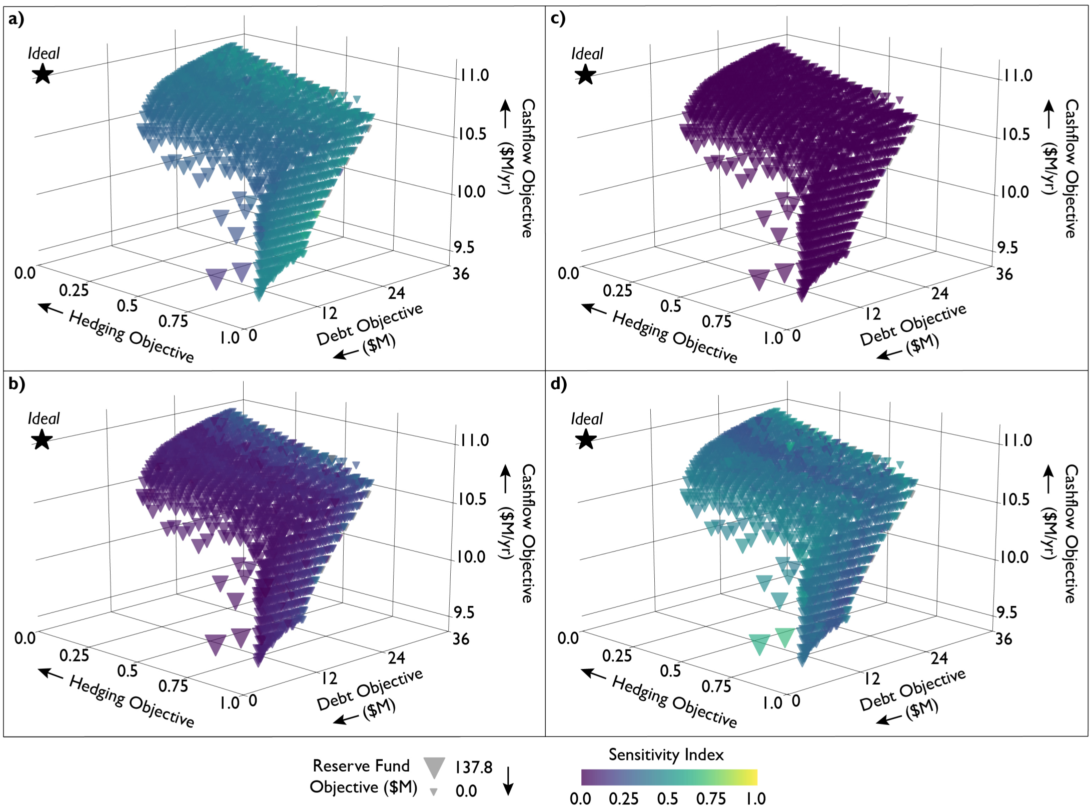

Figure S6. Entropic sensitivity indices, relative to withdrawal/deposit decision, for the reserve fund balance (a), debt (b), power price index (c), and incoming cash flow (Cash Flow 2) (d).

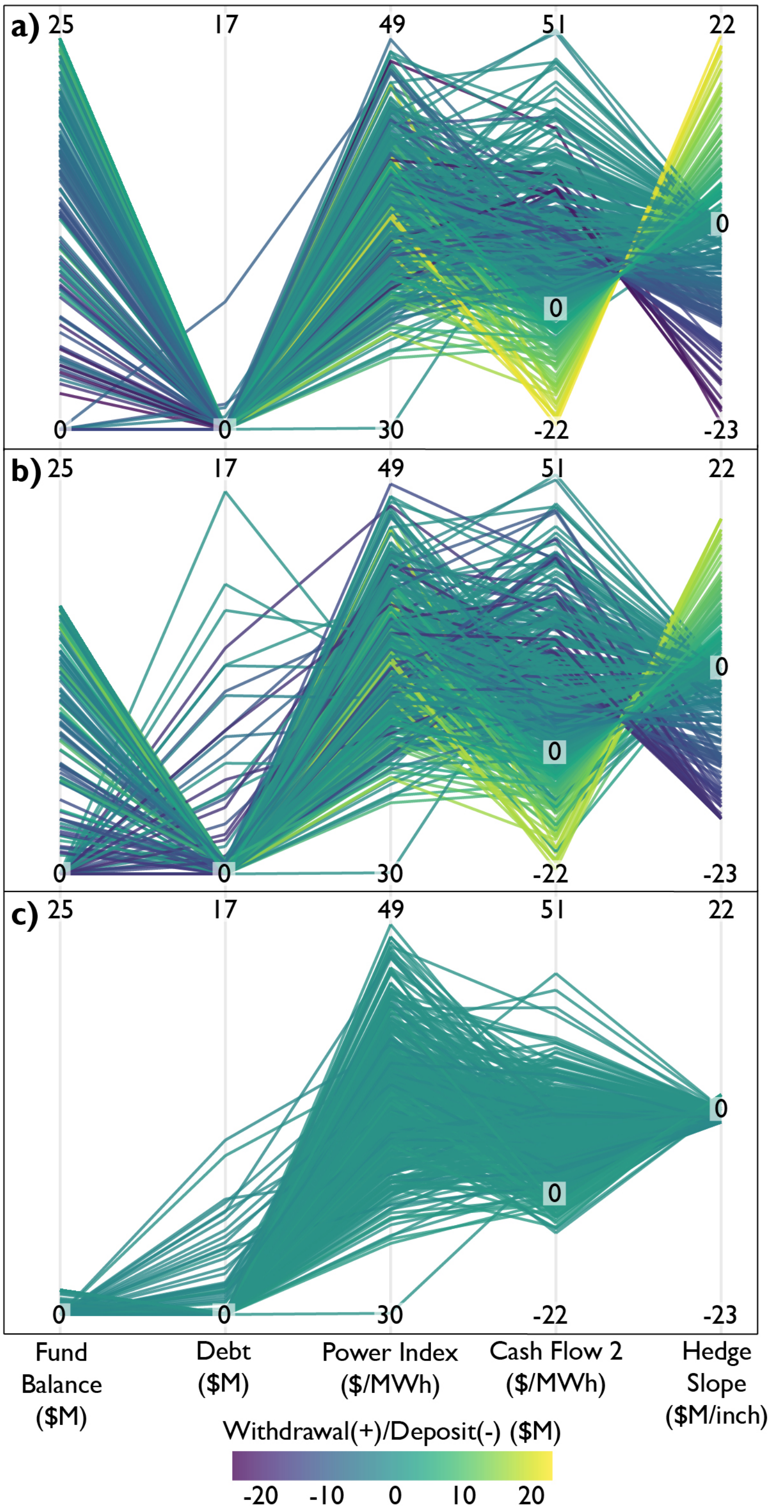

Figure S7. Withdrawal/Deposit control policy visualization for three chosen policies in Figure 8 and rows 4-6 of Table 2 in the main text. The policies are chosen due to their high sensitivity (with respect to the hedging control policy) to the reserve fund (a), debt (b), and power price index (c) information.

References

Hamilton, A. L., Characklis, G. W., & Reed, P. M. (2020). Managing financial risk tradeoffs for hydropower generation using snowpack-based index contracts. *Water Resources Research*, *56*, e2020WR027212. doi: 10.1029/2020wr027212